Physics – Uspekhi **43** (3) 259 – 282 (2000)

REVIEWS OF TOPICAL PROBLEMS PACS number: 78.60.Mq

Sonoluminescence

M A Margulis

DOI: 10.1070/PU2000v043n03ABEH000455

Contents

1. **Introduction** 259
2. **Influence of the main parameters on the multibubble SL flux** 260
3. **Spectra of multibubble SL** 260
4. **Basic theories explaining the occurrence of SL in response to cavitation fields** 262
   4.1 Thermic theories of cavitation; 4.2 Electric theories of cavitation
5. **Single-bubble sonoluminescence** 268
   5.1 Main peculiarities of single-bubble SL; 5.2 Duration of the flash of single-bubble SL; 5.3 Spectra of single-bubble SL; 5.4 Influence of inert gas additions on single-bubble SL; 5.5 Maximum temperature in a solitary cavitation bubble; 5.6 Shock waves in the cavitation field
6. **General analysis of experimental and theoretical data** 275
   6.1 Mechanism of multibubble SL; 6.2 Mechanism of single-bubble SL
7. **Conclusions** 279

References 280

Abstract. The current status of knowledge of the sonoluminescence mechanism is reviewed. It is shown that the origin of sonoluminescence in multibubble cavitation fields is best described by the local charging theory of cavitation bubbles. For certain acoustic field configurations, a single stably pulsating cavitation bubble develops, which differs from its 'ordinary' counterparts in a number of respects, and whose sonoluminescence is a thermal effect in contrast to the luminescent glow of the ensemble of 'cold' cavitation bubbles. A model of single-bubble sonoluminescence is proposed, which includes the additional resonance absorption of energy by a solitary cavitation bubble in a symmetric acoustic field. The mechanisms of some single-bubble effects are as yet not clear.

1. Introduction

Weak glow arising in a liquid in response to acoustic vibrations was discovered in 1934 by Frenzel and Schultes[1] [1]. This phenomenon which was given the name sonoluminescence (SL) has attracted considerable attention due to its versatility, inconsistency and the interesting and sometimes enigmatic discoveries made every so often (see, for instance, reviews [2 – 12]). In this paper we consider the basic works devoted to ultrasound SL thus breaking the 'tradition' of recent years which has been to present material in rather a peculiar way (see, for example, Refs [11, 12]), i.e. firstly to refer to the pioneering work [1] of 1934 and then to discuss only the papers published after the discovery of single-bubble SL in 1992 [13].

Numerous experiments have demonstrated that SL arises in a liquid only in the presence of cavitation. Relying on the fact that usual quenchers of luminescence in a liquid had no effect on SL, while those of the gas phase suppressed it, Harvey [14] concluded that the emission of light in response to ultrasound takes place inside cavitation bubbles filled with gas. At present this viewpoint is held by most researchers. Studies on the mechanism of SL origin have provided rather valuable information on physico-chemical parameters inside the cavitation bubble, the dynamics of their changes and the nature of cavitation.

Considerable progress in the studies of SL has been made comparatively recently, when Crum and his colleagues [22, 13] found that SL can be attained in a focusing cylindrical acoustic chamber with a single stable levitating cavitation bubble which does not have to be additionally fragmented. Barber and Putterman [23] devised a spherical single-bubble acoustic chamber. A bubble fixed at a certain point and pulsating for a long time made more versatile and unambiguous studies into the nature of cavitation and SL feasible. Thus, one could use a picosecond laser technique, follow uninterruptedly the motion of the surface of a solitary cavitation bubble, determine the bubble radius and the rate of motion of its wall with a high precision, and fix the initial moment and duration of SL impulsive flare with a high

M A Margulis N N Andreev Acoustics Institute,
Russian Academy of Sciences
ul. Shvernika 4, 117036 Moscow, Russian Federation
Tel. (7-095) 126 90 53. Fax (7-095) 126 84 11
E-mail: antok@akin.ru

Received 18 January 1999
Uspekhi Fizicheskikh Nauk **170** (3) 263 – 287 (2000)
Translated by G N Chuev; edited by A Radzig

[1] In some papers, especially in those published in recent years, the discovery of SL is accredited to Marinesco and Trillat [35], who observed darkening of photoplates on exposure to ultrasound. However, this effect might not be photochemical, as it could be caused by the chemical action of ultrasound, colloid – chemical or thermal effects in the swelled photoemulsion, etc. Therefore, the authors of Ref. [1] were the first directly to observe luminescence of a liquid in response to ultrasound after adaptation of an eye to darkness.

resolution. The emission of light from a solitary cavitation bubble visible to the naked eye did not cast any doubt that single-bubble SL as well as the multibubble is produced by a pulsating cavitation bubble. Even the first experiments on single-bubble SL demonstrated the considerable peculiarity of this phenomenon as compared to 'ordinary' multibubble SL. Questions arose of the reasons of this difference, of whether single-bubble SL is a fundamentally different phenomenon to be considered independently, and, finally, what the perspectives for the use of single-bubble SL in science and technology are. The opening up of these important and interesting directions of investigations has attracted many new researchers (worked previously on other problems) into this field and undoubtedly raised the level of experimental and theoretical treatment. In this connection the second part of our review deals with the works devoted to single-bubble SL.

2. Influence of the main parameters on the multibubble SL flux

Temperature and pressure as well as their rates of changes have a great effect on the SL flux U. As the temperature rises, the SL flux decreases due to the increased pressure of saturated vapor inside the cavitation bubble. It was generally believed that SL could be detected in water at temperatures not exceeding $T \sim 65\,^{\circ}\mathrm{C}$ [24] (Fig 1a, curve *1*), however the authors of Ref. [25] demonstrated that it can be observed even in boiling liquid (Fig. 1a, curve *2*) when ultrasound acts for a short time to avoid degassing. The dependence of U on pressure has a maximum which shifts to the region of an increased hydrostatic pressure p_{h} as the intensity of ultrasound rises (Fig. 1b). SL takes place not only at increased but also at decreased pressures; for fast evacuation of the chamber [25] it occurs at $p_{\mathrm{h}} \sim 15$ mm Hg, when cavitation bubbles cannot collapse at all.

The frequency of acoustic vibrations influences the SL flux [4, 9] and spectrum [26]. The SL spectrum was recorded at various frequencies: in high (300 – 1500 kHz [28 – 30]), medium (1 – 100 kHz [28 – 31]) and low (7 – 800 Hz [4, 9]) frequency ranges (in terms of the classification made in Ref. [27]). Sonoluminescence was also observed under the action of low-frequency sound and infrasonic vibrations [32], as well as in the case of hydrodynamic cavitation [33, 34].

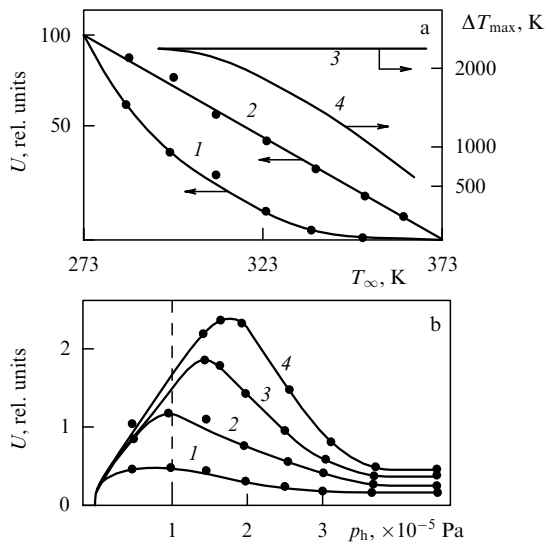

Figure 1. Dependence of the SL flux U on temperature in liquid (a) in water at 20 kHz (curves *1* and *2*) and on the maximum calculated temperature increase $\Delta T_{\max}$ in the cavitation bubble (curves *3* and *4*), and on hydrostatic pressure (b) at intensities: *1* — 0.8; *2* — 1.6; *3* — 2.4; *4* — 3.2 W cm^{-2}.

SL arises not only in water but also in various organic solvents [15, 16] and polymers at temperatures only slightly exceeding the melting point [17]. Ultrasonic glow was detected in mercury [18] and in melts of various metals [19]. According to paper [8], ultrasonic glow in metals at temperatures higher than T_{melt} differs from the SL effect; it arises as a result of charging when liquid metal is detached from the surface of a transparent window. The intensity of the glow is affected by inorganic [14] and organic [20] compounds, substances with a high pressure of saturated vapor [21], dissolved gases [20, 21], etc. In the presence of gases, the SL intensity decreases through the series: Xe > Kr > Ar > Ne > He > H_2. Some substances, such as CS_2, Br_2, CH_3I, CCl_4 [14] considerably enhance the SL intensity in water, but cannot produce SL on their own.

3. Spectra of multibubble SL

Initially, the SL spectra were studied with the use of photoplates [36, 37] which only enabled one to record a continuous spectrum varying from the lower bound of the photoplate sensitivity in the visible range to the ultraviolet one. Nowadays these works are only of historical interest. The studies carried out by Taylor and Jarman [28] presented the next step in the investigations of the spectra of multibubble SL. Using a monochromator with a high light-gathering power, a photomultiplier, and a recording device with a PC, they obtained SL spectra in water and aqueous salt solutions saturated with Xe, Kr, Ar, O_2 and air at the frequencies of 16 and 500 kHz. Some of the water spectra are depicted in Fig. 2a. For comparison, we also presented SL spectra obtained in water by Didenko et al. [38, 39] and a luminescence spectrum caused by hydrodynamic cavitation [33]. In water, the SL spectrum contains several bands corresponding to:

(1) deactivation of excited H_2O^* molecules with a maximum at 270 nm;

(2) emission of electronically excited hydroxyl OH^* according to the reactions

$$H_2O(B) \rightarrow H + OH^*(^2\Sigma^+) \rightarrow H_2O + OH(X) + h\nu$$

with maxima at 280, 310, 318, and 340 nm;

(3) radiative deactivation of vibrationally excited H_2O with a wide band extending into 380 – 600 nm;

(4) recombination radiation

$$H + OH \rightarrow H_2O(B) \rightarrow [H \ldots OH \ldots M]^* \rightarrow H_2O + M + h\nu\,.$$

When a complex is electronically excited, the luminescence peaks at 270 nm, and when it is vibrationally excited the maximum is reached at 380 nm.

If a solution contains luminol or other substances which give rise to chemiluminescence on reaction with radicals formed in the ultrasonic field, this solution will also exhibit sonochemiluminescence with a wide emission spectrum peaking at 430 nm [40] (Fig. 2a, curve *6*). This sonochemiluminescence is characterized by comparatively high duration of emission, which is of the order of 10^{-2} s. In the presence of

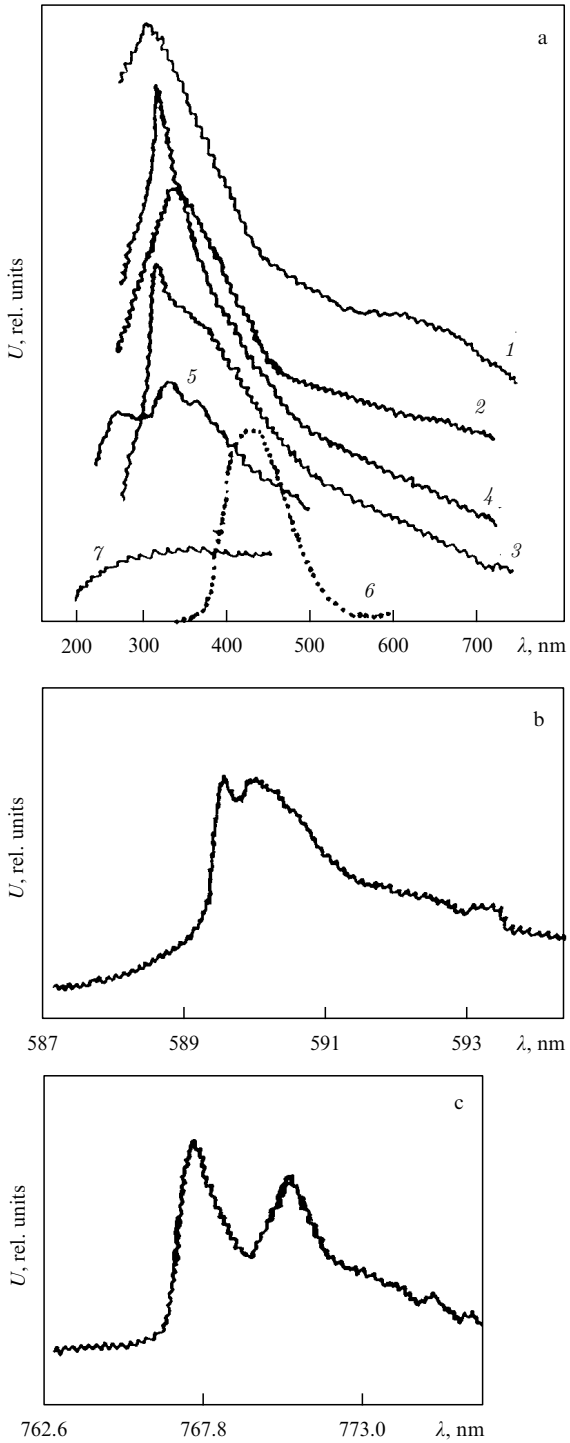

Figure 2. SL spectra in (a) water saturated with various gases: *1* — 500 kHz, air; *2* — 16 kHz, air; *3* — 500 kHz, Xe; *4* — 16 kHz, Xe [28]; *5* — 337 kHz, Ar [26]; *6* — water solution of luminol [156]; *7* — water and mixture of air and 17% Ar at hydrodynamic cavitation [33]; (b) NaCl solution, and (c) KCl solution.

acceptors of hydroxyl radicals, such as NO_3^- ions, the OH^* bands and the H_2O^* continuous spectrum disappear. In this case the low-frequency limit of the emission spectrum becomes rather sharp, about 424 ± 8 nm [41, 42]. SL spectra of concentrated salt solutions show intense lines of the corresponding metals. Salts substantially change the overall emission spectrum of SL. For example, in a water solution of NaCl saturated with argon at 500 kHz, the intensity of the D-line of Na is 6 times higher than that of the continuous component at the same wavelengths. At 16 kHz, the intensity of the D-line is approximately 200-fold higher, the intensity of the continuous spectrum itself increasing 17-fold in the red spectral region and 3-fold at the maximum [28]. The spectral doublet lines of sodium and potassium were recorded [43, 44] due to the high resolution (~ 0.8 nm) of the SL spectra of these metals (Fig. 2b,c).

In a recent work [45], Kuhns and his colleagues used a highly sensitive cooled detector to investigate multibubble SL of a solution containing 1 M NaCl. They observed considerable broadening of the Na D-line toward the red spectral region as compared to that in a flame containing NaCl. This effect cannot be caused by increased pressure in the gas phase, which would have resulted in a symmetric Lorenzian distribution [46]. The asymmetry of the sodium D-line is due to Rayleigh broadening toward the red region of the spectrum [47] and nonequilibrium light emission under inelastic scattering of emitted light in water. Therefore, this part of the spectrum cannot provide any information on the temperature of the emitter. The elementary processes of dissociation and excitation of MX halogenides are described by the equation

$$\mathrm{MX} \xrightarrow{\Delta E} \mathrm{M}^* + \mathrm{X}\,, \quad \mathrm{M}^* \longrightarrow \mathrm{M} + h\nu_{\mathrm{m}}\,. \tag{1}$$

In the first reaction, the molecular dissociation and excitation of the product occur as a single elementary process and are not stimulated by any other collisions, i.e. the process is primary. According to Ref. [48], metal ions residing on the walls of a cavitation bubble produce a line spectrum through a mechanism similar to the glow of impurities on the walls of shock tubes. This model does not imply any artificial assumptions such as the formation of cumulative jets, as in Refs [29, 30], or the appearance of microdrops inside the cavitation bubble at the moment of its collapse, as in Ref. [51].

In studies of the SL spectra of hydrocarbons, Suslick and his colleagues [29, 30] observed the emission of Swan bands (Fig. 3) caused by the $C_2(d^3\Pi_g - a^3\Pi_u)$ transition. According to their estimates, the vibrational and rotational excitations correspond to an effective temperature of about 5000 K. The SL spectra of many organic compounds [29, 30] obtained in

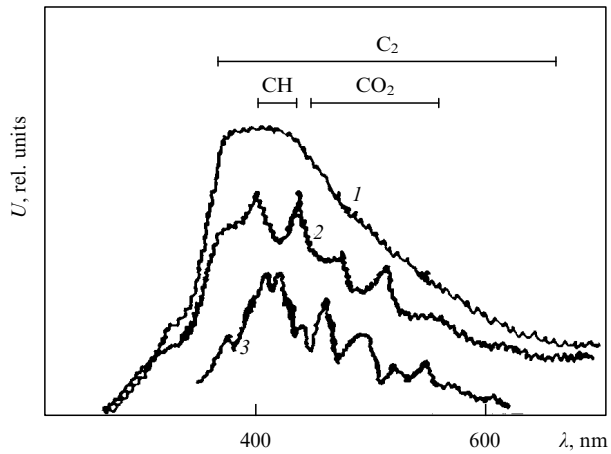

Figure 3. SL spectra of various organic compounds: *1* — dodecane in an oxygen atmosphere at 4 °C; *2* — dodecane in the mixture (O_2 + 90 % Ar) [52], and *3* — nitroethane in an argon atmosphere [30].

an oxygen-free atmosphere contain Swan bands which are similar to the emission spectra of hydrocarbons in flames, plasmas, shock waves, etc. The maxima at 563.6, 516.5, 473.7, and 438.2 nm were found to be due to the $d^3\Pi_g \rightarrow {}^3\Pi_u$ transitions with $\Delta v = -1,\ 0,\ +1,\ +2$, respectively. Note that finding the cavitation bubble temperature from the spectral data [150] always involves assumptions of the existence of a local thermodynamic equilibrium between various radiative terms and the average mass temperature of the steam – gas mixture in the cavitation bubble, however, this assumption is rather difficult to substantiate. In a recent work Suslick [177] estimated more precisely the maximal temperature and pressure in the cavitation bubble, synthesizing the emission spectra of SL by computational methods. The temperature was found to be about 3000 – 5000 K, while the pressure was about 1000 atm, however, these conditions can be obtained not only for the adiabatic collapse of a cavitation bubble but also as a result of electrical breakdown inside the bubble.

4. Basic theories explaining the occurrence of SL in response to cavitation fields

4.1 Thermal theories of cavitation

At present there are two main groups of theories to explain the mechanism of SL, namely, 'thermal' and 'electric' ones. In 1950, Noltingk and Neppiras [55], studying the dynamic equations for cavitation, developed a thermal theory of 'hot spot', which proposes that at the moment of adiabatic collapse[2] of the cavitation bubble, the temperature inside the bubble rises to about 10^4 K and that the arising light is the equilibrium radiation of a black body. Some other versions of the thermal theory were also proposed. According to the Griffing hypothesis [56], the light emission in water is caused by recombination of H and OH radicals generated as a result of thermal homolytic dissociation of water. Jarman [57] considered a collapsing cavitation bubble as a microscopic shock tube where shock waves are focused during the bubble compression. In this case, the light emission should be thermal. Thus, an explanation was provided for light emission arising at the instant of collapse of a cavitation bubble filled with gas (which is similar to black-body radiation), thermal dissociation of liquid vapor, generation of high-pressure pulses and shock waves, etc. Our analysis [4] of the holograms presented in Ref. [58] showed that shock waves rather seldom arise in a multibubble case in response to ultrasound. However, according to more recent results obtained by Lauterborn [59] for laser cavitation, shock waves can reasonably often be generated upon the single collapse of a bubble.

The Rayleigh – Plesset (RP) equation describing the dynamics of pulsations of cavitation bubbles in an incompressible liquid can be written as [24, 60, 61]

$$r\ddot{r} + \frac{3}{2}\dot{r}^2 + \frac{1}{\rho}\left(p_\infty - p_v - p_g + \frac{2\sigma}{r} + \frac{4\mu\dot{r}}{r}\right) = 0\,, \qquad (2)$$

where r is the bubble radius, ρ, σ, and μ are the density, surface tension, and viscosity of the liquid, respectively, p_∞ is the pressure in liquid, while p_g and p_v are the partial pressures of gas and vapor in the cavitation bubble. The pressure in the liquid is equal to

$$p_\infty = p_h - p_M \sin\omega t\,, \qquad (3)$$

where p_h and p_M are the hydrostatic pressure and the amplitude of the sound pressure, and ω is the circular frequency of acoustic vibrations. According to Refs [24, 62], the sum of p_g and p_v in the bubble whose radius varies from the initial value r_0 to r is expressed as

$$p_g + p_v = \left(p_{g0} + \frac{2\sigma}{r_0}\right)\left(\frac{r_0}{r}\right)^{3\gamma} + p_s\,, \qquad (4)$$

where γ is the ratio of heat capacities, p_{g0} and p_s are the gas pressure for the initial bubble and the pressure of saturated vapor at constant temperature T_∞ of the liquid. Substituting (3) and (4) into (2), Noltingk and Neppiras (NN) obtained the following differential equation [24, 55]:

$$r\ddot{r} + \frac{3}{2}\dot{r}^2 + \frac{1}{\rho}\left[p_h - p_M \sin\omega t - p_s + \frac{2\sigma}{r} + \frac{4\mu\dot{r}}{r} - \left(p_{g0} + \frac{2\sigma}{r_0}\right)\left(\frac{r_0}{r}\right)^{3\gamma}\right] = 0\,. \qquad (5)$$

However, the maximal temperature in the cavitation bubble, calculated by the RP or NN formulas which were derived with the use of Eqn (4) turns out to be independent of the temperature T_∞ of liquid (see Fig. 1a, curve *3*). Analysis of the reasons for the inadequacy of these formulas, performed by Margulis and Maksimenko [63], showed that the equilibrium condition on the surface of a collapsing cavitation bubble should be changed. Accounting for the partial pressure of vapor in the cavitation bubble is rather important. Actually, indefinitely high temperatures can be obtained for an empty cavitation bubble. Equation (4) proposes that the evaporation and condensation rates are infinitely high.

We showed in Ref. [63] that formula (4) should be changed. According to the Hertz – Knudsen equation, the critical velocity v_{cr} of the bubble wall above which evaporation and condensation can be neglected, is rather small and makes up about 5.8 m s^{-1} at $T_\infty = 393$ K [24, 168]. At the intermediate stage of bubble expansion the velocity of the bubble wall motion can be 6 m s^{-1} or higher. At the same time the average velocity of this expansion is equal to $2R_{max}f$, where f is the frequency of acoustic vibrations and does not exceed 2 m s^{-1} at maximal bubble radius $R_{max} = 40$ μm and $f = 26$ kHz. Hence, at the point of maximum expansion the vapor pressure inside the bubble is equal to the saturation vapor pressure. When the bubble compresses, the velocity of its wall greatly exceeds the critical value v_{cr}, i.e. the liquid and vapor have no time to evaporate and condense and the vapor behaves as gas. Therefore, as is shown in Refs [63, 142], formula (4) for the sum $p_g + p_v$ is approximately valid only at the stage of cavitation bubble expansion. At the stage of

[2] The term 'collapse' is not absolutely correct to describe what happens to a cavitation bubble, since we mean not a true collapse when the bubble completely disappears along with the bubble – liquid interface, but merely a process of rather fast compression when the bubble's radius reaches its minimum and the density of the steam – gas mixture inside the bubble becomes close to the fluid density. The cooled compressed gas occurring in the bubble serves as a nucleus for expanding cavitation bubble. The true collapse of a cavitation bubble is possible either in the case of vapor cavitation when the bubble is only filled with vapor of the liquid [9, 152] or in a liquid without any gases.

compression, a more correct formula reads as

$$p_g + p_v = \left[\left(p_{g0} + \frac{2\sigma}{r_0}\right)\left(\frac{r_0}{R_{max}}\right)^3 + p_s\right]\left(\frac{R_{max}^3}{r^3}\right)^\gamma, \quad (6)$$

where the product in the brackets is equal to the gas pressure $p_{g\,min}$ in the bubble of the maximum radius R_{max}; we also denote the expression in the brackets by p_{ad}. Thus, according to the NN equation (5) $p_{ad} = p_{g\,min}$, but more correctly $p_{ad} = p_{g\,min} + p_s$. Calculating the maximal temperature T_{max} in the cavitation bubble and using (6) instead of (4) in equation (5), we obtain the dependence of T_{max} on T_∞ which fits the experimental data (see Fig. 1a, curve *4*). Thus, the numerical experiments carried out in Ref. [63] showed that at the stage of 'collapse' the vapor does not manage to condense and behaves as gas[3].

As is shown in Refs [72, 142], nonideal gas effects in a cavitation bubble have a considerable influence on the behavior of a bubble at the stage of compression in the acoustic field. In these works, the van der Waals equation of state was used to describe adiabatic compression of a bubble. According to numerical estimates, the internal (van der Waals) pressure of gas can be neglected and the dependence of the gas pressure in a cavitation bubble on the bubble radius takes the form

$$p_0 \approx p_{ad}\left(\frac{R_{max}^3}{r^3 - b_1^3}\right)^{\gamma_p}, \quad (7)$$

where p_{ad} corresponds to the sum in the brackets of Eqn (6), b_1 is the radius of the sphere in which the distribution of steam – gas molecules inside the bubble corresponds to the most dense package and

$$b_1^3 = \frac{3nb}{4\pi},$$

where b is the van der Waals constant, and n is the number of moles of steam – gas mixture in the bubble. The adiabatic index γ_r of real gas is described by the formula [142]

$$\gamma_r = \gamma + \frac{2apn}{C_V RT^2} \quad (8)$$

(here γ is the adiabatic index of ideal gas, a is another van der Waals constant, C_V is the heat capacity of ideal gas, and R is the gas constant). The calculations [142] showed that the adiabatic index is approximately equal to that in ideal gas, i.e. $\gamma_r \approx \gamma$ as the bubble collapses in moderate sound fields ($p_м < 15$ atm).

Taking into account the terms dealing with nonideal behavior of steam – gas mixture and slow rates of condensation and evaporation, we obtain the following modified equation [different from NN equation (5)] for the compression of a cavitation bubble [9]:

$$r\ddot{r} + \frac{3}{2}\dot{r}^2 + \frac{1}{\rho}\left[p_h - p_м \sin\omega t + \frac{2\sigma}{r} + \frac{4\mu\dot{r}}{r} - \right.$$
$$\left. - (p_{g\,min} + p_s)\left(\frac{R_{max}^3}{r^3 - b_1^3}\right)^\gamma\right] = 0. \quad (9)$$

[3] It is shown in Ref. [71], however, that for low intensities of pulsations and comparatively slow expansion of a cavitation bubble, the rate of phase transitions is rather high and the vapor partial pressure corresponds to p_s, unlike in the case with intense and moderate acoustic fields.

Neglecting changes in the sound pressure during the short time of the bubble compression, i.e. putting $p(t) \sim \langle p_м \rangle$, and ignoring viscosity and surface tension effects, the authors of Ref. [142] integrated (9) and found the minimal radius of the bubble to be

$$r_{min} = \left(b_1^3 + \frac{R_{max}^3}{A^{1/(\gamma-1)}}\right)^{1/3}, \quad (10)$$

where the parameter A characterizes the sound field intensity. As in the case with an ideal steam – gas mixture, one has

$$A = 1 + \frac{p_h + \langle p_м \rangle}{3p_{ad}}, \quad (11)$$

where $\langle p_м \rangle$ is the sound pressure averaged over the time of the bubble compression (as a rule it is considerably less than $p_м$). Physically, formula (10) implies that the total volume of gas molecules inside the bubble should be added to the bubble volume determined by the formulas for ideal gas. According to Eqn (10), at $A > A_{cr} \equiv R_{max}/b_1$ (which can take place in moderate sound fields), the nonideal gas effects have considerable influence on the dynamics of the bubble. Using the condition of conservation of the number of particles in the steam – gas mixture inside the bubble during its compression, the authors of Ref. [142] found the parameter A_{cr} to be

$$A_{cr}^3 \approx \frac{RT_\infty}{p_{ad} b}. \quad (12)$$

The calculations using Eqn (12) showed that at $T_\infty = 300$ K and pressure $p_{ad} = 1$ atm, a bubble of radius R_{max} cannot conceptually compress more than 8.8 times after production of 'infinitely high pressure'. The strongest compression for multibubble cavitation undergoes a vapor bubble whose volume may decrease by a factor of 32 [142].

If we use the adiabatic model for the steam – gas mixture in the bubble, the nonideal effects do not influence T_{max} and p_{max}. At the same time these effects can substantially increase the heat exchange between the bubble and liquid as compared to that in the ideal gas, since the bubble surface averaged over time increases considerably at the final stage of compression when the temperature and pressure in the bubble are close to the maximum values. The expression for the maximum rate of motion of the bubble wall at $A < 3A_{cr}/4$ and $\gamma = 4/3$ is written as

$$\dot{r}_{max}^2 \approx \frac{2p_{ad}}{3\rho}\left[\frac{3A/4}{1 + (3A/4A_{cr})^3/4}\right]^4, \quad (13)$$

i.e. the maximum velocity of travel of the bubble wall decreases $[1 + (3A/4A_{cr})^3/4]^2$ times with regard to the nonideality of the steam – gas mixture. In intense sound fields at $A \gg A_{cr}$ we have

$$\dot{r}_{max}^2 \approx \frac{2A_{cr}^3(p_h + \langle p_м \rangle)}{3\rho};$$

this maximal velocity is independent of pressure in a resonant bubble. The above formulas are valid as long as the compressibility of liquids can be neglected, i.e. when $\dot{r}_{max} < c$, where c is the speed of sound. If we use $\dot{r}_{max} = c$ in calculations by formulas for the ideal gas, then in a bubble filled with air the nonideal gas effects decrease the maximum velocity twice or more [142].

According to Ref. [147] where the collapse of cavitation bubbles was studied with due regard for heat exchange, the maximum temperature and the maximum velocity of travel of the bubble wall decrease approximately twice, while the maximum pressure decreases by an order of magnitude.

Equations for pulsations of a cavitation bubble with regard for the compressibility of liquids were obtained by Herring and Flynn [24], Kirkwood and Bethe [64], and Keller and Miksis [65 – 67]. However, the role of compressibility in the dynamics of a bubble turns out to be considerably less than follows from these equations, since the above-mentioned effects substantially decrease the rate of the bubble compression. In none of the considered models of cavitation bubble collapse is there a set of equations which could take into account all the relevant factors such as the interactions between bubbles, compressibility of liquids, deformations of bubbles, heat and mass exchange and phase transitions in a collapsing bubble at temperatures greatly exceeding the critical ones. Some principal difficulties should be overcome to consider the appearance of supercritical parameters, the realization of a thermodynamic cycle bypassing the critical point, the rate of increase in the temperature $(\dot{T})_{\max} \sim 10^{10} - 10^{12}$ K s^{-1} and continuous changes in the mass and composition of the steam – gas mixture. Most of the works devoted to the dynamics of cavitation deal with a spherically symmetric problem and ignore the origin of deformations under fast compression of the bubble, loss of its stability and its splitting into small fragments [68, 69].

To account for deformations in studies of the dynamics of nonspherical bubbles, Prosperetti and Seminara [70] considered the RP equation [of the type of Eqn (2)], where the bubble radius is described by the sum

$$r = \bar{r}(t) + a(t)\, Y_{nm}(\theta, \varphi)\,, \tag{14}$$

where $a(t)$ is the deviation of the bubble surface from the spherical radius $r(t)$ in the normal direction, and $Y_{nm}(\theta, \varphi)$ are the spherical harmonics for the deformed surface of the bubble. The authors dealt only with rather small shape distortions: $|a_n/r| \ll 1$. However, even in this case Eqn (2) with r determined by (14) turns out to be extremely complicated. Thus, the maximum temperature and pressures as well as the partial pressures of gas, vapor of liquid and products of their dissociation cannot be accurately evaluated from the data of numerical solutions.

4.2 Electric theories of cavitation

Until recently, electrical phenomena accompanying cavitation were the least understood. Levshin and Rzhevkin [130] proposed that SL is caused by electrical charges arising on the cavitation bubble walls due to an effect similar to the balloelectrical (Lenard) effect; however, a theoretical treatment of this hypothesis was lacking.

According to the theory put forward by Frenkel' [131], the cavitation cavity in liquid initially has a lens shape and uncompensated electrical charges of opposite sign are generated at the moment of breaking of the liquid as a result of fluctuations in the distribution of ions occuring in the liquid on the bubble walls. The fluctuation of the charges is proportional to the square root of the total number of ions $Cs\delta$ in the arising cavitation bubble. For singly-charged ions, this uncompensated charge is equal to

$$Q = \mathrm{e}\sqrt{Cs\delta}\,, \tag{15}$$

where e is the electron charge, C is the number of ions in the unit volume, s and δ are the cross section and thickness of the cavity. The electric field intensity of such a capacitor is

$$E = \frac{4\mathrm{e}}{r_{\mathrm{c}}}\sqrt{C\delta}\,, \tag{16}$$

where r_{c} is the cavity radius. According to Frenkel's estimates, at $C = 10^{18}$ cm^{-3}, $\delta = 5 \times 10^{-8}$ cm, and $r_{\mathrm{c}} = 10^{-4}$ cm, the field intensity is about $E \sim 600$ V cm^{-1}, which corresponds to the critical value E_{cr} for a pressure in the cavity not exceeding ~ 2 kPa. However, the author of Ref. [132] raised some serious objections against Frenkel's theory [131].

(1) The value $C = 10^{18}$ cm^{-3} is too high for water (it corresponds to an excessively high ion concentration $\sim 1.7 \times 10^{-3}$ M dm^{-3}). For example, in water at pH = 7 one finds $C_{\mathrm{H}^+} = 10^{14}$ cm^{-3} and $E \sim 6$ V cm^{-1}, which is much less than the critical value at atmospheric pressure, E_{cr}. For other liquids where SL can arise, the ion concentration is several orders of magnitude yet less than in water and $E \ll 1$ V cm^{-1}.

(2) For breakdown and avalanche ionization to take place, the thickness of Frenkel's cavity δ should greatly exceed the mean free path λ in the cavity, but at $E \sim 600$ V cm^{-1} the breakdown requires a pressure under 2 kPa, which corresponds to $\lambda \sim 10^{-3}$ cm $\gg \delta$.

(3) The cavity thickness $\delta \sim 5 \times 10^{-8}$ cm is approximately equal to the kinetic diameter of a water molecule. Therefore, Frenkel's cavity can only arise in a homogeneous liquid not containing microbubbles, which just serve as nuclei for cavitation. However, in such a liquid with moderate ultrasound intensity, cavitation cannot take place at all.

Harvey [14] related the SL origin to the appearance of electrical charges on the cavity walls, assuming the electrical breakdown to occur at maximum compression of the bubble. However, he did not provide any quantitative substantiation for this viewpoint. This approach cannot be considered satisfactory either [132], since at the moment of compression the pressure and hence E_{cr} are also at a maximum. Besides, the electric field intensity in a spherical cavity, on the surface of which the electrical charges are uniformly distributed, is equal to zero.

Degrois and Baldo [133] proposed that anions adsorbed on the cavitation bubble surface are neutralized, and some excess electrons are formed due to induced polarization of gas molecules inside the bubble. For fast compression, a high gradient of charge density is produced on the interface, and microdischarges directed towards the liquid arise in the bubble. As is shown in Ref. [132], the authors of Ref. [133] did not estimate the electric field intensity and rates of several concurrent processes such as electric conductivity, electron diffusion, recombination, etc. It is not clear either why charges of opposite sign are produced on the bubble walls where anions of the same charge are adsorbed. The electric field intensity in the spherical bubble charged by ions of the same charge is equal to zero as is the case with the Harvey bubble [14]. The authors of Refs [73, 132] demonstrated that the results of work [133] are in conflict with the experimental data.

In 1985, Margulis [74] developed a theory of local charging of cavitation bubbles, which was in agreement with most of the experimental results (see below Section 6.1). We will consider the ideas underlying the theory in view of their significance and novelty (some works were published in the last 2 – 3 years). In essence, they are as follows. A double electrical layer arises at the interface of the cavitation bubble in liquid. According to the Stern – Helmholtz scheme, we can

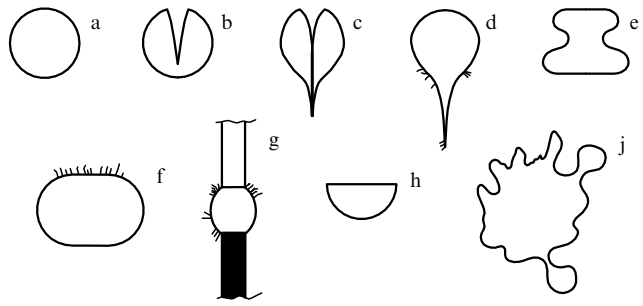

Figure 4. Various shapes of cavitation bubbles in liquid: (a) spherical shape; (b) and (c) radial cumulative jets [68]; (d) formation of local microheterogeneities on the surface of cumulative jets [68]; (e) circular cumulative jets [69]; (f) surface microheterogeneities on flattened cavitation bubbles [76]; (g) local microheterogeneities on the surface of a cavitation bubble formed via the explosion of a tungsten filament [79]; (h) lens-shaped cavitation bubbles under the action of an acoustic field of frequency 80 Hz [77], and (j) loss of stability and formation of single or several fragmentation cavitation bubbles.

consider conditionally two regions of the layer, a dense part which is close to the surface of the double layer, and a diffusive distant part where adsorption forces can be neglected and ions are mobile in liquid. Independently of the origin of cavitation, the interface is quickly and repeatedly refreshed when the cavitation bubble moves. The surface potential may be induced either due to orientation effects or owing to the presence of impurity ions. Impurities may be in such small amounts ($\sim 7 \times 10^8$ cm^{-3}) that they cannot be detected experimentally. They have no effect on the physicochemical properties of the liquid, but take part in the appearance of the surface charge. The formation of the double electrical layer at the interface is a common property of liquids (not necessarily water).

The uncompensated electrical charge is brought about by acoustic flows which flush away some fraction of the diffusive double layer. We can arbitrarily consider three basic acoustic flows: Schlichting small-scale vortex flows in a viscous boundary layer; Rayleigh flows whose scale corresponds to the acoustic wavelength, and Eckart large-scale flows caused by the action of an acoustic beam [75]. As a result of pulsations, the cavitation bubbles lose the stability of their spherical shape, become deformed and, eventually, disintegrate. Analyzing electrical phenomena, we should consider not only spherical bubbles (Fig. 4a), but also various deformations such as the appearance of radial (Figs 4b, c, and d) [68] and circular (Fig. 4e) [159] cumulative jets; the occurrence of surface roughness (Fig. 4f) [76] and lens-shaped cavitation bubbles (Fig. 4h) [77], as well as their disintegration with the formation of several fragmentation bubbles (Fig. 4j). Surface roughnesses occur widely not only at cavitation produced by ultrasound but also at cavitation occurring in hydrodynamic flows [78], at the explosion of a tungsten filament in liquid (Fig. 4g) [79], or on exposure to a laser beam [68] and so forth. Our analysis [4] of rapid holographic film frames obtained by Ebeling [58] showed that most of the cavitation bubbles in an ultrasonic field of frequency 22 kHz are deformed and their surfaces are covered with sprouts, asperities, microheterogeneities, etc. In general form, the surface charging of cavitation bubbles can be considered only for two limiting cases, i.e. for their fragmentation [4, 9, 27, 74, 80, 81] and deformation (without fragmentation) [85, 83].

The splitting of cavitation bubbles occurs with the detachment of a fragmentation bubble (Fig. 5). The movement relative to the interface, which is caused by a liquid flow, involves not the whole double ion layer but only a portion with the coordinate $x > x_s$ (where x_s is the sliding boundary). The electrokinetic potential ζ is the surface potential at the point $x = x_s$, and for $x < x_s$ the charges hold near the liquid surface. The quantity of electricity transferred by the liquid flow from the bubble surface into the liquid per unit time (electric current) is equal to [74]

$$I = \pi\varepsilon\varepsilon_0 \zeta \frac{r_n^2}{l\mu} \Delta p \,, \tag{17}$$

where ε is the permittivity of the medium, ε_0 is the dielectric constant, μ is the viscosity coefficient, r_n and l are the radius and length of the neck at the moment of the bubble splitting. For a bubble to be fragmented, the acoustic field should overcome the pressure gradient [81]

$$\Delta p = \frac{\sigma}{r_n} + \frac{16}{3}\pi^2 f^2 a\rho \frac{r^3}{r_n^2} + 12\pi\mu a f \frac{r}{r_n^2} + \frac{Q^2}{8\pi^2\varepsilon\varepsilon_0 r_n^2 l^2} \,, \tag{18}$$

where f and a are the frequency and the amplitude of acoustic vibrations, and Q is the uncompensated electric charge. The terms in the right side of Eqn (18) correspond respectively to overcoming the surface tension force, the pressure necessary to disturb the bubble surface, the Stokes force, and the electrostatic repulsion between like charges on the walls of the contracting bubble neck. These effects prevent fragmentation of the cavitation bubble, and a part of the energy required

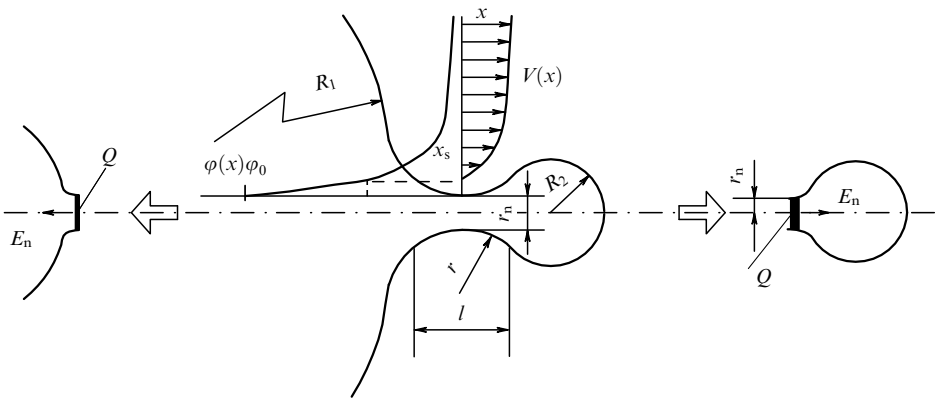

Figure 5. Scheme of changes in the surface potential, electric field intensity and local charge on splitting of a cavitation bubble.

to overcome them can be accumulated and transformed into the energy of electric discharge. The uncompensated charge is equal to

$$\mathrm{d}Q = (I - i)\,\mathrm{d}t\,, \tag{19}$$

while the conduction current should satisfy the following condition

$$i \leqslant \frac{Q}{2\varepsilon\varepsilon_0\lambda_0}\,\frac{r_\mathrm{n}}{\delta}\,,$$

where δ is the effective thickness of the double electric layer, and λ_0 is the electric conductivity of the liquid. In Ref. [81], an equation was derived for the process of charging and concurrent charge sinking due to electric conductivity such that

$$\mathrm{d}Q = \left[\frac{\pi\varepsilon\varepsilon_0\zeta}{\mu l}\left(\sigma r_\mathrm{n} + \frac{16}{3}\,\pi^2 f^2 a\rho r^3 + 12\pi\mu a f r\right) + \frac{\zeta Q^2}{8\pi\mu l^3} - \frac{Q}{2\varepsilon\varepsilon_0\lambda_0}\,\frac{r_\mathrm{n}}{\delta}\right]\mathrm{d}t\,. \tag{20}$$

The analytical solution to this equation can be written as [81]

$$Q \approx \frac{A}{2C}\exp\left(-\frac{C}{2}\,t\right), \tag{21}$$

where we use the following notation

$$A \equiv \frac{\pi\varepsilon\varepsilon_0\zeta}{\mu l}\left(\sigma r_\mathrm{n} + \frac{16}{3}\pi^2 f^2 a\rho r^3 + 12\pi\mu a f r\right),$$

$$C \equiv \frac{1}{2\varepsilon\varepsilon_0\lambda_0}\,\frac{r_\mathrm{n}}{\delta}\,.$$

At the moment of cavitation bubble splitting, the charge held on the surface of the neck is sorbed on a small spot whose radius approximates that of the neck, r_n. The normal component of the electric field strength in the vicinity of this charged spot on the surface of the main or fragmentation bubble is equal to [81]

$$E_\mathrm{n} = \frac{Q(0)}{2\pi\varepsilon_0 r_\mathrm{n}^2}\,. \tag{22}$$

At the moment the cavitation bubble disintegrates, the uncompensated electric charge occurring on the surface of the neck is evenly divided between two fragments (Fig. 5). Our calculations showed that at $t = 0$ the charge of the spot on the cavitation bubble is equal to $Q(0) = 8.5 \times 10^{-14}$ C, while the local charge density found with respect to cross section of the neck is $\langle\sigma(0)\rangle = 2.8 \times 10^{-2}\ \mathrm{C\,m^{-2}}$. The characteristic time for sinking of this charge due to electric conductivity is about 2.8×10^{-7} s and much shorter than the period of acoustic vibrations. The time during which the electrical breakdown occurs can be estimated from the equation of an electron motion under the action of a constant electric force $-\mathrm{e}E_\mathrm{cr}$, the electron velocity varying from 0 to $\mathrm{e}E\tau/m_\mathrm{e}$ on the mean free path λ, where m_e is the electron mass, and τ is the time between electron collisions. Then the time necessary for the breakdown to occur is equal to [169]

$$\tau_\mathrm{br} \sim 10\tau \approx 10\sqrt{\frac{2m_\mathrm{e}\lambda}{\mathrm{e}E_\mathrm{cr}}}\,.$$

For $\lambda = 10^{-7}$ m and $E_\mathrm{cr} = 3 \times 10^6$ V m^{-1} we obtain $\tau_\mathrm{br} \sim 10^{-11}$ s. Thus, the characteristic breakdown time determined by the time during which the electron avalanche develops is many orders of magnitude shorter than the characteristic time of charge relaxation due to electric conductivity.

The critical electric field intensity E_cr depends on the nature of the gas in a cavitation bubble, pressure $p = p_\mathrm{g} + p_\mathrm{v}$ in the bubble, temporal changes in the pressure, temperature T, humidity δ_0 (or p_s), etc. This dependence can be written as [84]

$$E_\mathrm{cr} = E_\mathrm{cr}^0\,\frac{(p/p_\mathrm{st})^m (T/T_\mathrm{st})^n}{K_\delta}\,. \tag{23}$$

Here $K_\delta \sim 0.9$, $m = n = 1$ and E_cr^0 corresponds to standard experimental conditions, i.e. pressure $p_\mathrm{st} = 1$ atm, temperature $T_\mathrm{st} \sim 293$ K, and absolute humidity of air $\delta_0 = 11\ \mathrm{g\,m^{-3}}$. For typical parameters of cavitation bubbles in water at 20 kHz, the electric field intensity is $E_\mathrm{n} = 1.5 \times 10^9\ \mathrm{V\,m^{-1}}$ which is many orders of magnitude greater than the critical value ($E_\mathrm{cr} \sim 3 \times 10^6\ \mathrm{V\,m^{-1}}$). Since the critical field intensity E_cr is proportional to pressure p (the Townsend law), the electric discharge can occur in a cavitation bubble with high probability even at a pressure of hundreds of atmospheres. In this case the mean free path λ is much shorter than the minimal bubble radius r_min and one more condition for the occurrence of avalanche ionization is fulfilled:

$$\lambda \ll r\,.$$

The deformation of cavitation bubbles takes place even at rather low sound pressures [82], and as is shown in Refs [83, 85, 87], this deformation is accompanied by surface charging. The types of deformation of initially spherical cavitation bubbles are highly diversified (see Fig. 4). Notice that the electric charge is at maximum near the surface with the greatest curvature. In the general case it will suffice to consider only two types of disturbances [153]:

(1) local disturbances whose cross section decreases as the distance from the undisturbed surface grows; the surface of such disturbance is approximated by a paraboloid of revolution;

(2) local disturbances resulting in the formation of a waist (neck) between the primary and fragmentation bubbles; the surface of such a disturbance is approximated by a hyperboloid of one sheet.

It is common for a bubble to develop several disturbances at a time, but we can consider only one at which the electric field intensity is maximum and the electrical breakdown is the most probable. The potential U of the disturbed surface is equal to ψ, and $\psi > \zeta$, but underestimating the result we can take $U \sim \zeta$. At the close of the disturbance we have for the potential $U_0 \sim \mu_\mathrm{p}(\beta)\zeta$, where $\mu_\mathrm{p}(\beta)$ is the amplification coefficient of the potential at the point of the greatest curvature [83].

Deformations of a parabolic shape with a base radius $r_\mathrm{p} \ll r$ are of frequent occurrence. In the coordinate system x, z where the end of the disturbance asperity (point O) coincides with the origin of coordinates, the axially symmetric cross section of the paraboloid is described by $z = ax^2$, where the axis z coincides with the paraboloid one. The electric potential at the point O, induced by an element of the charge $\mathrm{d}Q = \sigma_0\,\mathrm{d}S$, where $\mathrm{d}S$ is an element of the disturbed surface

at the point (x, z), is equal to [83]

$$\mathrm{d}U_0 = \frac{\sigma_0\,\mathrm{d}S}{4\pi\varepsilon\varepsilon_0\sqrt{x^2+z^2}}\,, \tag{24}$$

where σ_0 is the surface charge density. The potential at the point O is written as

$$U_0 = \frac{\sigma_0}{\varepsilon\varepsilon_0 a}\left(\sqrt{1+a^2r^2}-1\right) = \frac{\sigma_0 r_\mathrm{p}^2}{\varepsilon\varepsilon_0 H}\left(\sqrt{1+\left(\frac{H}{r_\mathrm{p}}\right)^2}-1\right),$$

where H is the height of the asperity. Thus, at $H \gg r_\mathrm{p}$ we have

$$\sigma_0 = \frac{\varepsilon\varepsilon_0\zeta\mu_\mathrm{p}}{r_\mathrm{p}}\,,$$

where $\mu_\mathrm{p}(H/r_\mathrm{p})$ is the coefficient taking into account the increase in the potential at the top of paraboloid due to nonuniform distribution of charges. The electric field intensity E_0 at the point of the greatest curvature, i.e. at the endpoint of paraboloid (point O), comprises the electric field intensity E_p produced by the paraboloid and the electric field intensity of the remaining part of the bubble, which is calculated as the electric intensity of a sphere E_sph minus the electric intensity E_d induced by a disk at the point O. Our calculations showed that at $H \gg r$ the latter is small: $E_\mathrm{d} \ll E_\mathrm{sph} \sim E_\mathrm{p}$. Therefore we arrive at [83]

$$E_0 \approx E_\mathrm{sph} + E_\mathrm{p} \approx \frac{\varepsilon\zeta}{r}\left(\frac{1}{1+(H/r)^2}+\frac{\mu_\mathrm{p} r}{r_\mathrm{p}}\right). \tag{25}$$

Thus, the maximum electric intensity arising at the disturbance endpoint is determined by the bubble radius r, the dimensions of disturbance r_p and H, the electrokinetic potential and the dielectric constant of liquid. In principle, the electric field intensities E_sph and E_p can be commensurable. Note that the electric intensity is at a maximum when r_p and r are at a minimum, while the dielectric constant ε is a maximum. When a cumulative jet is directed inside the bubble (Figs 4b and c), the maximum electric intensity at the point with greatest curvature (endpoint of the paraboloid) is described by Eqn (25). But at the point O lying inside the sphere the electric intensity E_sph is equal to zero. Therefore, when the disturbance is directed inside the cavitation bubble, the electric intensity is considerably lower than in the case with outwardly directed cumulative jet. According to Ref. [83], the electric intensity produced by deformations of the cavitation bubble is much lower than that arising during splitting of the bubble. Electrical breakdown of the bubble saturated with air can occur when the bubble expands, viz. when the pressure in the bubble is lower than that of the atmosphere:

$$p_\mathrm{g} + p_\mathrm{v} \leqslant \frac{E_0}{E_\mathrm{cr}}\cdot 760 = \frac{4.1\times 10^5}{3\times 10^6}\cdot 760 = 104\ \mathrm{mm\ Hg}\,.$$

For example, the electrical breakdown is possible in argon when the pressure in the cavitation bubble is about 620 mm Hg, since $E_\mathrm{cr}^0 \sim 5\times 10^5\ \mathrm{V\,m^{-1}}$ in this case, i.e. it is lower than in the air. At the stage of compression (without collapse) the electrical breakdown of the cavitation bubble saturated by air takes place even at increased pressure $p_\mathrm{g} + p_\mathrm{v} \leqslant 8.2$ atm.

Deformations in the shape of a hyperboloid arise when forming the neck of the minimum radius r_n and length l between initial and fragmentation bubbles. This process always precedes the splitting of the bubble and hence its probability is high. To find the electric potential at the surface of the cavitation bubble neck, the authors of Ref. [85] used the Lamé method [86]. The field potential in proximity to the neck surface is determined in this case by a function of the parameter r_n: $U = U(r_\mathrm{n})$ and satisfies the Laplace equation $\Delta U = 0$. The electric field intensity produced by the bubble neck at the point (x, y, z) in proximity to the neck surface in the gas phase is equal to [85]

$$E(r_\mathrm{n}, d) \approx \frac{Qd}{4\pi\varepsilon_0 l r_\mathrm{n}^2}\,, \tag{26}$$

where d is the distance between the origin of the coordinate system and the plane tangent to the considered surface at the point (x, y, z). Equation (26) takes into account a nonuniform charge distribution over the neck surface and allows one to calculate the electric intensity at any of its points near the place of its maximum narrowing. The potential at the neck surface is found to be [85]

$$U = \frac{Q\sqrt{c^2-r_\mathrm{n}^2}}{4\pi\varepsilon_0 l c}\left[\ln\frac{c+\sqrt{c^2-r_\mathrm{n}^2}}{r_\mathrm{n}}\right] + \zeta\,. \tag{27}$$

The charge at the neck surface is given by

$$Q = 2\pi(\varepsilon-1)\varepsilon_0 l\zeta\varkappa\frac{R_0}{r}\,, \tag{28}$$

where the parameter $\varkappa$ characterizes the neck surface curvature:

$$\varkappa = \sqrt{\frac{1+4(R_0^2-r_\mathrm{n}^2)^2}{R_0^2 l^2}}\,.$$

Thus, we have [85]

$$E_\mathrm{max} = \frac{(\varepsilon-1)\zeta\varkappa R_0}{2r}\,. \tag{29}$$

Prior to fragmentation of a cavitation bubble, there develops a neck of relatively long length l and short boundary radius R_0; in water $\varkappa \approx 1.04$, $Q \approx 1.9\times 10^{-15}$ C, $E_\mathrm{max} \approx 4\times 10^5\ \mathrm{V\,m^{-1}} \ll E_\mathrm{cr}$ and electrical breakdown is unlikely. For circular cumulative jets $Q \approx 4\times 10^{-15}$ C, $E_\mathrm{max} \approx 2\times 10^7\ \mathrm{V\,m^{-1}}$, and the probability of neck electrical breakdown goes high.

The local intensity of the electric field is a maximum at minor disturbances of the cavitation bubble, which are hardly resolved, for example, with an optical microscope. The results obtained suggest an alternative mechanism for local charging of cavitation bubbles and accordingly the occurrence of SL, which could hardly have been proposed *a priori*. Prolonged pulsations of cavitation bubbles in an acoustic field can give rise to microscopic disturbances on the bubble surface. These surface disturbances make up the points of localization of the maximum electric intensity and microdischarges can occur there.

Until recently no suggestions have been made as to the mechanisms of the so-called prethreshold SL [87]. It may be proposed that weak light emission arising in the liquid before the appearance of a developed cavitation ($\sim 10^{-3}\ \mathrm{W\,cm^{-2}}$) is produced by electric microdischarges which occur in the regions of microscopic disturbances at the surface of cavitation bubbles upon their prolonged pulsation without splitting.

The authors of Ref. [88] observed a phase shift of the SL and its emission in both the half-periods of acoustic vibrations under the action of ultrasound in liquid saturated with xenon. This effect can be accounted for by various mechanisms of charging of the cavitation bubbles [85]: some of the bubbles experience electrical breakdown when they expand and develop local deformations, others — at the stage of their compression followed by splitting.

5. Single-bubble sonoluminescence

5.1 Main peculiarities of single-bubble SL

In previous sections we were concerned with 'ordinary' multibubble cavitation and SL. Now we pass on to consideration of numerous works devoted to single-bubble SL, which came under the scrutiny of science after it was discovered by Crum and his colleagues [13, 22] and has ever since attracted considerable attention of researchers. Single-bubble cavitation develops as follows. First, a cluster of pulsating cavitation bubbles arises in the focal region. Due to the Bjerknes force this cluster little by little attracts other bubbles pulsating with the same phase. After a short time a solitary stable (as regards the phase and intensity of SL flashes) cavitation bubble arises, which pulsates for a long time (up to several hours). Single-bubble SL turned out to be very sensitive to sound pressure, concentration and type of dissolved gas, type and temperature of liquid and other parameters. Barber and Putterman [23, 89, 160] found and investigated considerable differences in the behavior of single- and multibubble systems, such as

(1) The duration of light emission is rather short in the case of single-bubble SL.

(2) Single-bubble SL is very sensitive to the addition of minor amounts of inert gases.

(3) The spectrum of single-bubble SL differs fundamentally from that of cavitation field SL.

(4) The maximum temperature in the cavitation bubble can be as much as 25 000 – 50 000 K [12], 100 000 K or still higher [124]. At such temperatures the emission spectrum agrees satisfactorily with that of a black body. Single-bubble sonoluminescent emission is much more intense than that of multibubble SL; it has a blue color and is visible to the naked eye [11].

(5) The moment of the SL flash corresponds to the minimum radius of the cavitation bubble.

(6) Intense shock waves can be initiated in single-bubble systems [11].

The problem that first arises in studies of SL and cavitation is to understand the nature (electrical or thermal) of SL in multi- and single-bubble cavitation fields. Another fundamental problem is to find out whether ordinary and single-bubble SL have the same origin, or are quite different phenomena though both types of light emission arise in response to ultrasonic waves.

SL can be produced by a solitary cavitation bubble without its splitting only when the bubble pulsations are synchronised with symmetrical vibrations of the chamber. Since shape distortions of a spherical cavitation bubble are rather small in a single-bubble chamber and the maximum ratio between the major and minor axes of the ellipsoidal bubble does not exceed 2.0 during the process of compression [11], the electrical effects on the bubble surface seem to be of little importance, however, these points call for further investigation. It may be suggested that a solitary bubble emits light, in principle, due to thermal effects, while an ensemble of cavitation bubbles produce cold luminescent emission.

In principle, the thermal mechanism of single-bubble SL can be described by equations obtained in the dynamic theory of cavitation. Recall that these equations were derived for a solitary cavitation bubble, i.e. for a system where the interactions between bubbles are not taken into account. Therefore, the thermal theory of cavitation after a series of impressive improvements (see the following sections) can be applied to single-bubble systems, and the main physical and mathematical apparatus of the theory may be tentatively thought of as adequate (see Section 4.1). Now let us consider in greater detail the experimentally established peculiarities of single-bubble SL.

5.2 Duration of the flash of single-bubble SL

The duration t_s of the sound-driven flash of the single-bubble SL has been studied by a number of researchers. The authors of Refs [11, 161] found it to be < 50 ps. At the same time Moran and his colleagues [143] using a streak camera with a high time resolution (about 10 ps) concluded that $t_s < 12$ ps. However, this result should be refined, since according to papers [11, 125] these authors measured the duration of a background pulse rather than the duration of the SL pulse, because the intensity of light emission is rather low. The experimental data on t_s are very important to reveal the mechanism of SL occurrence. Works [113 – 115,118, 119, 124, 158] and some others provide a theoretical explanation for the origin of such short SL pulses (see Section 6). The authors of Ref. [161] measured the temporal characteristics of the SL flash in a single-bubble system with a photomultiplier and found the building-up and fall times of the signal to be 0.5 and 1.4 ns. These times are shorter than those obtained by us in a multibubble system (1 and 8 ns, respectively) [112] [4] and result in a duration t_s of the SL pulse at a half intensity (as in Ref. [161]) of less than 3 ns.

Conducting the experiment with a photomultiplier, the authors of Ref. [161] used the radiation of a pulsed laser with a pulse duration $t_l = 34$ ps in lieu of the source of a single-bubble emission and obtained approximately the same pattern on a screen of an oscilloscope. Relying on this finding they concluded that the duration of a SL pulse is shorter than 50 ps. However, this conclusion is not sufficiently grounded. Actually, we can make a thought experiment and use a pulsed laser of the sufficient power with $t_l \sim 1$ fs as a control source of emission. Then, due to the long time required for the development of an electron avalanche at the dynodes of the photomultiplier, we will obtain identical shapes of the SL and laser-driven pulses. But this must not lead us to conclude incorrectly that $t_s < 1$ fs!

Gompf and his colleagues [125] carried out the most careful experiments on determining the duration of an SL pulse in single-bubble systems. They used the emission of an ultraviolet laser with rather short pulses ($t_l \sim 0.3$ ps) as a control source of radiation and applied a more sophisticated measuring system with two photomultipliers and a multi-

[4] Referring to our works [31, 48, 96, 164], the authors of Ref. [161] incorrectly cited our estimate of the duration of the SL pulse as $t_s < 10$ μs. However, in these works we were dealing with multibubble SL and the time intervals found are shorter than 10 ns (see above). Besides, if we evaluate the duration of the SL pulse at a half intensity then, according to our experimental data, $t_s < 3$ ns in multibubble systems.

channel analyzer to detect the resolution time in the system, which was found to be about 30 ps. This time is much shorter than t_1 (in contrast to that found in Ref. [161]). This significant refinement allowed them to determine the duration of a single-bubble SL pulse under various experimental conditions. At low concentration of dissolved gas and low sound pressure, single-bubble SL emission is not visible to the naked eye and $t_s \sim 100$ ps, while at sound pressure 1.25 atm and oxygen concentration $C_g = 3.3\,\%$ the duration is $t_s = 260$ ps [125], i.e. approximately an order of magnitude less than the level of temporal resolution achieved with an ordinary photomultiplier (which is about 1 – 3 ns in the case of multibubble SL [112, 161]). Taking into account more recent data [54, 125, 162, 163], we can believe that the duration of a single-bubble SL pulse is equal to 100 – 350 ps and depends on the concentration of dissolved gas. Clearly, at low gas concentration the light emission is very weak, and only the peak portion of the SL pulse can be obtained experimentally. Thus, the duration of a single-bubble SL pulse is more accurately detected at enhanced (within some limits) concentrations of dissolved gas.

The authors of Refs [49, 91] without sufficient grounds believe that the time t_s characterizes sonoluminescence both in an ordinary cavitation field and in single-bubble ones, however, this viewpoint is not supported by any experimental evidence. To answer the question of whether a single-bubble SL presents some effect in its own right or it is ordinary SL where only one bubble pulsates, Giri and Arakeri [170] investigated the duration of SL pulses for multibubble, single-bubble, and a few bubbles SL [183]. The authors of Ref. [170] used single-bubble SL to 'calibrate' the duration of SL pulses and demonstrated that the transition from the single-bubble SL to SL caused by a few bubbles is accompanied by a sharp (180-fold) increase in the light pulse duration and in doing so the measurements showed that $t_s = 10$ ns at high sound pressures, and $t_s = 70.6$ ns at low ones. An important point is that unlike the case with single-bubble SL, the shape of a pulse of SL produced by a few bubbles becomes asymmetrical (sharp increase and monotonic decrease as in our work [112]). Bands in the multibubble SL spectrum (for example, the D-line of Na) are broaden at an enhanced sound pressure.

Weninger and his colleagues [155] studied the SL of a solitary cavitation bubble in contact with a solid surface. The properties of such a hemispherical pulsating bubble (such as the SL intensity, SL spectra of hydrocarbons, etc.) were found to be intermediate between those of a multibubble cavitation field and a single levitating bubble.

Thus, extensive experimental evidence has been accumulated testifying that single-bubble SL is an independent physical effect.

5.3 Spectra of single-bubble SL

Single-bubble SL spectrum differs from that of an ensemble of cavitation bubbles in the following features:

— its spectrum extends from 700 to 190 nm and further to the ultraviolet region [89] (Fig. 6);

— the intensity of the emission spectrum of a single bubble containing He, Ne, and Ar increases continually as the wavelength decreases down to 200 nm [89];

— the intensity of the spectrum of single-bubble SL arising in a water solution of He or Ar monotonically grows as $\sim \lambda^{-2.5}$ with decrease of the wavelength, while in aqueous solution of Xe a wide maximum at $\sim$ 300 nm is recorded [134];

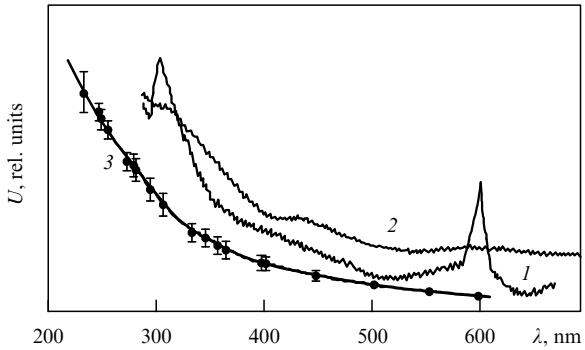

Figure 6. SL spectra: *1* — aqueous solution of NaCl in an ordinary cavitation field; *2* — aqueous solution of NaCl in a focused single-bubble system [49]; *3* — water in a single-bubble system (dots) and emission spectrum of a black body at 25 000 K (line) [89].

— under spectral resolution of 1 nm, any spectral lines of OH*, recombination bands of H + OH and others are not revealed in the spectrum of single-bubble SL occurring in water [89] (compare, for example, Figs 2a and 6);

— the most intense band, viz. Na D-line, is missing from the single-bubble SL spectrum observed in sonolysis of an aqueous solution of NaCl (Fig. 6) [49, 50][5];

— the Swan bands produced by excited carbon molecules are not found in the spectrum of single-bubble SL in dodecane [90] saturated with Xe (unlike in the case with multibubble SL [29, 30, 52]).

These experimental facts suggest that the origin of single-bubble SL differs from that of 'ordinary' multibubble SL. Barber and Putterman [11] concluded that monotone character of the single-bubble SL spectrum is due to the emission of the black body and differs considerably from the multibubble SL spectrum which includes a lot of intense emission bands. For example, the authors of Refs [29, 30, 41 – 44] obtained the spectra of multibubble SL for water, aqueous solutions, hydrocarbons, etc., containing many typical bands indicated above (see Section 3). Multibubble SL spectra are in no way the spectra of a black body. In Section 3 we discussed the mechanism of nonequilibrium luminescent emission produced by excited atoms, molecules and radicals occurring inside pulsating cavitation bubbles.

Some researchers [49, 91] do not see any principal difference between the mechanisms of single- and multibubble SL. To 'bridge' these processes, they try to find conditions at which the properties of single-bubble systems virtually do not differ from those of ordinary multibubble ones. Thus, they remove the cavitation region from the emitter, or saturate the bubbles with one or another gas, or do something of the kind. Clearly, at low sound pressures the spectrum of multibubble SL is smooth and diffusive; it does not include any pronounced bands of OH* or other substances and, therefore, cannot be compared with the spectrum of the single bubble SL. Needless to say, the data of such experiments do not lead us to conclude that single- and multibubble SL are similar phenomena. On the other hand,

[5] The authors of Ref. [49] investigated single-bubble SL in a 0.1 M solution of NaCl, while in the works on the spectra of multibubble SL the most intense band (D-line of Na) was observed at much higher concentrations of NaCl of about 2 M. Therefore it seems appropriate to carry out additional investigations of the spectra of single-bubble SL in concentrated solutions of NaCl.

under certain conditions, for example, on exposure to pulsed focusing ultrasound or during multibubble cavitation one can attain rather high temperatures. Thus, Francescutto and his colleagues [92] obtained temperatures of about $T \sim 37\,000$ K with a focusing apparatus (the temperature was calculated from the spectrum of the black body).

5.4 Influence of inert gas additions on single-bubble SL

The concentration of dissolved gas in a single-bubble chamber has a pronounced effect on the flux U, which remains to be seen [11, 157]. As the concentration of gas C_g decreases from 75% to 16% of the saturation concentration of dissolved air, the flux U increases more than 10-fold [157]. At very low C_g, single-bubble SL does not take place at all [11]; as C_g rises, the duration of the SL pulse t_s also increases [125]: at $C_g = 0.5$ mg dm^{-3} (which corresponds to ~ 10 mm Hg) U is rather weak; as C_g rises, so does U, the SL becomes visible to the naked eye, the duration of the SL pulse also increases and, finally, at C_g close to the saturation concentration of gas in water at atmospheric pressure, we arrive at ordinary multibubble cavitation accompanied by relevant multibubble SL. Note that the flux U caused by the multibubble SL falls off as the gas concentration decreases [4]. For ordinary multibubble SL, the flux U continuously rises in the series He < Ne < Ar < Kr < Xe [9] as the ionization potential (I_{ion}) [or excitation energy (I_{ex})] of the dissolved gas decreases. The processes occurring in cavitation bubbles at the electrical breakdown are described by the reactions [4]:

$$\mathrm{Ar} -))) \longrightarrow \mathrm{Ar}^* ,$$
$$\mathrm{Ar}^* + \mathrm{H_2O} \longrightarrow \mathrm{H_2O}^* + \mathrm{Ar} ,$$
$$\mathrm{H_2O}^* \longrightarrow \mathrm{H} + \mathrm{OH} ,$$
$$\mathrm{H_2O}^* \longrightarrow \mathrm{H_2O} + h\nu .$$

Thus, the added inert gases are the first to become excited at the multibubble cavitation. Then the excited gas atoms transmit the excitation to water molecules due to the Frank – Hertz collisions of the second kind. The added atoms of He or Ne having high I_{ion} and I_{ex} (which are higher than those of water molecules) cannot take part in the charge exchange or excitation transfer processes. Therefore, for the multibubble cavitation the concentration of H_2O^* is maximum when water is saturated with Xe.

In the case of single-bubble SL, the addition of inert gas affects the SL flux in quite a different way. For example, the addition of about 1% of He, Ar or Xe into N_2, O_2, or argon-free air sharply increases the SL intensity (approximately by two orders of magnitude). However, further increase in the concentration of inert gas slightly (1.5 – 2-fold) decreases U [11, 134]. Thus, unlike in the case of multibubble SL, for single-bubble SL the dependence of U on the concentration of inert gas added is extremal. Besides, on addition of He to water the single-bubble SL flux and spectral temperature are maximal. It is still difficult to account for all the currently available experimental data.

In paper [144], it was proposed that on addition of argon to the air in a single cavitation bubble, the reactions proceed involving nitrogen and oxygen to form nitrogen oxides which react with excess water yielding $HNO_2 + HNO_3$, then irreversibly leave the bubble and are replaced by argon due to its rectified diffusion. Unlike in the case with multibubble cavitation, the maximum temperature at the moment of maximal compression of a solitary cavitation bubble can reach 50 000 K [11], 130 000 K [144] or still higher values. At such high temperatures, molecules of O_2, H_2, and H_2O can dissociate or be ionized with a high probability. According to Saha's formulas, double or triple ionization is the most probable at normal air density and a temperature of about 10^5 K. Therefore, over several periods oxygen and nitrogen molecules occurring in the bubble transform into nitrogen oxides which then produce ($HNO_2 + HNO_3$) in the presence of water excess. In so doing the solitary cavitation bubble is rather an effective chemical reactor where sound-chemical transformations different from those in ordinary cavitation fields take place [9, 182]. However, to substantiate this suggestion, we should clarify the following points:

— since air contains 78% N_2 and 21% O_2, then by stoichiometry rules after depletion of all oxygen the share of free nitrogen must be more than 63%;

— it is not clear how the processes of accumulation of inert gas occur in other systems such as pure oxygen, nitrogen, etc.;

— rectified diffusion is a slow process, and even if the air is completely replaced by argon, the maximum temperature may grow nearly 1.5 times due to the increase in γ, while the flux density of thermal emission increases as little as $1.5^4 \approx 5$ times; therefore it remains unclear why the flux U grows by nearly 2 orders of magnitude.

To answer these questions, we can propose the following improved model. In a cavitation bubble containing oxygen and water vapor (without nitrogen), the reactions proceed to produce H_2O_2. In a single-bubble system, hydrocarbons are decomposed into atoms and ions (unlike in the case with multibubble cavitation and, for example, reactions in a discharge tube). This circumstance, in our opinion, is the reason for the absence of Swan bands in the single-bubble SL spectrum of hydrocarbons [90]. For such processes to take place, temperatures of about 10^5 K and higher are required. We cannot yet explain the peculiarities of single-bubble SL spectra by other reasons.

The rectified diffusion of inert gases initially occurring in a bubble and also added to it may little by little change the gas content in a solitary bubble. As a result, in the steady state, almost all gases and substances with a high saturated vapor tension are 'burnt out' from a solitary cavitation bubble during several periods, and only the inert gases and copiously attending water vapor remain in the same amount. After that, despite the fact that the concentration of added inert gas is low (about 1%), the composition of a solitary cavitation bubble virtually jumpwise becomes steady, presenting mainly inert gases and water vapor.

A comparatively small decrease in U at high concentration of water-dissolved inert gas is probably due to the stability of pulsation of a solitary cavitation bubble, since at the maximum gas concentration (close to saturation concentration at atmospheric pressure) the bubble becomes unstable, deforms and disintegrates, giving rise to 'ordinary' multibubble cavitation.

To explain the maximum at ~ 300 nm in the case of the single-bubble SL of Xe, we propose that this sonoluminescence occurs in two steps: initially the blackbody radiation arises, all gases and vapor of liquids emitting in a similar manner, then the temperature decreases fast and the *luminescent emission of inert gases* is brought about.

The intensity of light emission is at maximum for gases with maximal ionization potential, which 'stored' the maximum excitation energy in a time of exposure to high

temperatures. The radiative deactivation of inert gases is determined in that case by the values of I_{ion} and I_{ex} of the corresponding gas. The maximum temperature and intensity of emission were observed in He; for other gases U decreases in the series: He > Ne > Ar > Kr > Xe, which is inverse to that revealed for the case of multibubble cavitation. To substantiate the model, we should take into account that at the maximum compression, the particle collision time is much shorter than the duration of a SL flash. Thus, the quenching time for electronically excited states is determined not by the radiative lifetimes of these states ($\sim 10^{-8}-10^{-4}$ s), but by the time of collisional deactivation, i.e. it is very short.

5.5 Maximum temperature in a solitary cavitation bubble

The phase and intensity of single-bubble SL are rather stable for a long time [11]. Some attempts to determine the maximum temperature in a collapsing solitary cavitation bubble were made by many authors, whose results vary by several orders of magnitude: 2500 K [13], 100 000 K [181], 50 000 K [11], 130 000 K [144], 3.5×10^8 K [166, 124], etc. Greenland [12], when considering the equation of state and dynamic equations of cavitation bubbles containing real gases, concluded that the steam – gas mixture inside the collapsing bubble acquires a high pressure and comparatively low temperature not exceeding 20 000 – 40 000 K. Therefore, he proposed that single-bubble SL exhibits not a high-temperature effect, but is governed by high pressure and the main problem is to understand why the temperature inside a solitary cavitation bubble is so small. In this connection Greenland believed that single-bubble SL may serve as a test system for studies in the field of the physics of high pressure. However, his hypothesis cannot account for many experimental facts such as:

— the reason for the differences between the single- and multibubble SL (see Section 5.1);

— the spectrum of single-bubble SL differs significantly from that of liquids highly compressed by shock; for example, intense Swan bands are experimentally examined in the spectrum of benzene at a pressure of hundreds of kilobars [178];

— the influence of small additions ($\sim 1\%$) of inert gases on single-bubble SL.

The abundant experimental evidence on single-bubble SL can be explained only on the assumption that the temperatures arising in single-bubble systems are much higher than those in multibubble cavitation.

Crum [50] supposed that the peculiarities of single-bubble SL are related to the fact that the acoustic field is symmetric and asymmetrical compression and deformations of a cavitation bubble are hampered. However, we think that there is another more important reason, namely, the energy supplied to the single bubble can be *many orders of magnitude higher* than that in the case of ordinary steady cavitation fields [95]. Let us neglect the linear absorption of acoustic energy by liquid and assume that in multibubble cavitation the bubbles of resonant size r_{res} absorb the main portion of the supplied energy. Then the time taken by cavitation bubbles to grow to the size r_{res} is determined by the average number i of pulsations. Therefore, we can believe that in multibubble systems the average acoustic energy E_1 supplied to a single resonant cavitation bubble during the period of acoustic vibrations is equal to $E_1 = Wi/n_\infty Vf$. While in the case of single-bubble system the corresponding acoustic energy is $E'_1 = W/f$. Hence one finds

$$\frac{E'_1}{E_1} = \frac{n_\infty V}{i}\,, \tag{30}$$

where n_∞ is the steady concentration of cavitation bubbles, V is the volume of the cavitation field, and W is the acoustic power. In normal cavitation fields, the steady concentration n_∞ can vary from 10^3 to 10^6 cm^{-3} [62, 96] and depends on the experimental conditions. In the focal region the ultrasound intensity can increase 10^3-10^6 times [97, 98] and more. At moderate ultrasound intensities the average number of pulsations i does not exceed 10 [4]. Therefore, according to Eqn (30) the energy ratio E'_1/E_1 can increase by 5 (!) orders of magnitude, which can dramatically change the behavior of cavitation bubbles [95]. However, we should specify which portion of the energy supplied to a solitary cavitation bubble is absorbed by it.

The above estimates of the energy supplied to a single cavitation bubble and resulting high temperatures are proved by the fact that the SL flux from a solitary stably pulsating bubble is visible to the naked eye and substantially exceeds the SL flux from an ensemble of many thousands of bubbles in the cavitation field. Notice that modern laser techniques applied to investigate experimentally the motion of a cavitation bubble in a single-bubble chamber allow researchers [11] to detect its essentially more effective extension to large dimensions and a faster compression as compared to the bubble compression in multibubble cavitation field.

In theoretical studies of the motion of a solitary cavitation bubble use is usually made of ordinary equations of the cavitation dynamics. However, this results in a paradoxical situation, i.e. the maximum sound pressure cannot exceed 1.5 atm [6] or 0.7 W cm^{-2}, which is the limit of stability for the cavitation bubble in a single-bubble chamber [13]. At the same time, it is necessary to explain high-temperature effects *which, in principle, cannot occur* inside the cavitation bubble at 0.3 – 0.7 W cm^{-2}. For example, Crum et al. [13] calculated the maximum temperature in the cavitation bubble to be about 2500 K. According to numerous publications, the intensities of about 0.3 – 0.7 W cm^{-2} are lower than the threshold of cavitation in settled water (of order several atmospheres), and the more so in degassed water [62].

The conclusions that at a sound pressure of 0.9 – 1.5 atm shock waves arise seem to be groundless, since for generation of even weak shock waves in a cavitation bubble filled with air, sound pressures exceeding 6 atm are required [9, 165]. The situation becomes even more complicated in view of the fact that if we managed to calculate such high temperatures, pressures, shock wave profiles, etc. for a single-bubble system at 0.7 W cm^{-2}, these parameters should have been the same for each of 10^3-10^5 (!) bubbles in 1 cm^3 of an ordinary cavitation field and, therefore, the system should have exhibited the same effects as we observed in the case of single-bubble SL. However, this is

[6] Studying cavitation processes in a single-bubble system, researchers usually deal with sound pressure on the chamber surface, which is easily measured. But it would be more correct to indicate the sound pressure in the center of the chamber in the vicinity of the cavitation bubble, which is hardly detected. This parameter more correctly describes the physical peculiarities of the cavitation process and can be used to compare the experimental data obtained under various configurations and dimensions of the unit.

in conflict with all the available experimental results (see Section 5.1). Thus, it is necessary to explain the reason for the peculiar behavior of single-bubble SL, when at low ultrasound intensities ($\sim 0.5\ \mathrm{W\,cm^{-2}}$) the system exhibits high temperature effects which are not observed (or show up only slightly) in multibubble acoustic fields even at high intensities ($\sim 100\ \mathrm{W\,cm^{-2}}$).

Some authors (see, for example, Refs [166, 167]), tried to calculate the maximum temperature, estimate the probability of the generation of shock waves, etc. in a single-bubble cavitation without noticing the peculiarities of single-bubble SL and the difference between the single- and multibubble SL effects. The authors of Ref. [167] calculated the temperature, using the general conservation equations of mass and angular momentum with additional boundary conditions instead of the usual dynamic equations for cavitation. In this case, the results found should not differ, in principle, from those obtained by the conventional methods using dynamic equations for cavitation, since the latter equations are derived from the same conservation equations of mass and angular momentum, etc. It is only essential for us that by defining the vapor pressure p_v as a function of T_∞, i.e. as a constant, the authors of Ref. [167] naturally obtained a high temperature exceeding 10^5 K. The values 354×10^5 K and 6×10^9 atm were found in Refs [166, 171] in a similar way. These results are due to the fact that the infinitely high temperature T_max and velocity $\dot{r}_\mathrm{max}$ are known to be obtained in an empty cavitation bubble. For the following reasons the partial vapor pressure must be taken into account by using Eqn (6) at the bubble compression stage, and Eqn (4) at the bubble expansion stage. The first reason is that evaporation and condensation rates are not high and these processes have no time to proceed even at velocities of the bubble wall exceeding $6\ \mathrm{m\,s^{-1}}$, and thus the vapor at these conditions behaves as a normal gas. The second reason is that at $p_\mathrm{s} = 0$ or $p_\mathrm{s} = \mathrm{const} \ll p_\mathrm{h}$, the maximum temperature T_max and correspondingly SL and other physico-chemical effects inside the bubble do not depend on temperature of liquid [63], thus contradicting the experimental data. The calculations of the maximum temperature are not detailed in paper [172], and we think that the explanation of single-bubble SL proposed by its authors is not convincing.

The authors of Ref. [145] studied single-bubble SL and analyzed the paradoxical situation at hand, and, as a result, derived *a new equation for the dynamics of a solitary cavitation bubble in the field of a spherical harmonic sound wave*. This equation takes into account the following most important effects: the focusing of the acoustic field, nonideal effects for a gas inside the bubble, various dependences of the partial pressure of fluid (water) vapor for the cavitation bubble compression and expansion stages, and a partial absorption of the energy of an incoming sound wave by the bubble. We considered the vibrations of the cavitation bubble in a field produced in a spherical chamber of radius R_ch by an acoustic emitter with a pressure distribution over the chamber surface described by Eqn (3). Then the solitary cavitation bubble is subjected to a spherical sound wave of amplitude

$$p_\mathrm{in} = \frac{p_\mathrm{M} R_\mathrm{ch}}{r} \exp(\mathrm{i}kr)\,,$$

where i is the imaginary unit, $k = \omega/c$ is the wave number (in the case of multibubble cavitation naturally $p_\mathrm{in} = p_\mathrm{M}$). Taking into account the reflected wave, we found that the sound pressure on the surface of a nonlinearly pulsating solitary cavitation bubble can be expressed for $kr \ll 1$ as

$$p_1(r) = p_\mathrm{M} R_\mathrm{ch}(1 - G)k + p_\mathrm{M} R_\mathrm{ch} \frac{G}{r}\,, \tag{31}$$

where $G(r)$ is a dimensionless parameter characterizing the portion of the energy of the incident acoustic wave, which is absorbed by the bubble. The exact dependence $G(r)$ can be derived by solving a complicated nonlinear problem. But in the case of single-bubble cavitation in contrast to multibubble cavitation, the amplitude of sound pressure may be approximated by the sum of the two terms, one of them being a function of the ratio R_ch/r. The estimates showed that under normal experimental conditions ($R_\mathrm{ch} \sim 3$ cm, $\omega \sim 10^5\ \mathrm{s^{-1}}$), the first term in Eqn (31) has the same order of magnitude as p_M at $G < 0.5$. At the same time, the second term in Eqn (31) at $G \approx 1$ greatly exceeds this value of p_M even when the radius of the cavitation bubble is about the maximum. With the account for the dependence of $G(r)$, instead of NN equation (5) or modified equation (9), we should use more complicated differential equation for describing single bubble cavitation [145]:

$$r\ddot{r} + \frac{3}{2}\dot{r}^2 + \frac{1}{\rho}\Bigg\{p_\mathrm{h} - \Bigg[p_\mathrm{M} R_\mathrm{ch} k(1 - G(r)) + p_\mathrm{M} R_\mathrm{ch} \frac{G(r)}{r}\Bigg] \sin\omega t + \frac{2\sigma}{r} + \frac{4\mu\dot{r}}{r} - (p_\mathrm{g} + p_\mathrm{v})\Bigg\} = 0\,, \tag{32}$$

where the sum $p_\mathrm{g} + p_\mathrm{v}$ is determined by Eqn (4) for the bubble expansion, and by Eqn (6) for its compression.

The resonant character of sound absorption by bubbles has been studied experimentally in many works and today is commonly accepted. Based on numerous experimental data, we believe that a solitary cavitation bubble can absorb the most of acoustic energy supplied to the bubble at the moment when its size is about the resonant one (or when the frequency of bubble natural vibrations is about the frequency of the acoustic field); in this case $G \to 1$ [145]. According to Ref. [173], the resonant cavitation bubbles absorb sound more intensively than they scatter it.

Analysis of the experimental data compiled in Refs [173, 179] demonstrated that the frequency dependence of the effective cross section of the energy absorption by a solitary cavitation bubble can be described by a Gaussian curve with a maximum corresponding to the resonant frequency of the bubble and a half-width of about ω_0/β [145]. The approximation of the data presented in Refs [173, 179] yields $\beta = 20$. Saxena and Nyborg [106] have investigated luminescence of a solitary floating cavitation bubble, caused by ultrasound in a cylindrical resonator. Following their data, the half-width of the distribution is approximately equal to $\omega_0/2$. Considering the resonant frequency ω_0 of the cavitation bubble to be dependent on the cavitation bubble radius through the Minnaert formula

$$\omega_0(r) = \sqrt{\frac{3\gamma(p_\mathrm{g} + p_\mathrm{v})}{\rho r^2}}\,, \tag{33}$$

the authors of Ref. [145] approximated $G(\omega/\omega_0)$ in the general form as an exponent with the maximum at $\omega_0 = \omega$ and a half-width ω_0/β:

$$G\left(\frac{\omega}{\omega_0}\right) \approx 1 \cdot \exp\left(-\frac{\beta|\omega - \omega_0|}{\omega_0}\right) \approx 1 \cdot \exp\left(-\beta\left|\frac{r\omega}{\sqrt{3\gamma(p_\mathrm{g} + p_\mathrm{v})/\rho}} - 1\right|\right)\,, \tag{34}$$

the pressure of steam – gas mixture in the bubble being described by Eqns (4) and (6) at the bubble compression and expansion stages, respectively. Calculating the parameters of the cavitation bubble in a single-bubble spherical chamber, we can neglect the compressibility of liquids at low sound pressures and use, for example, the NN equation, thus arriving at solution of the following differential equation:

$$r\ddot{r} + \frac{3}{2}\dot{r}^2 + \frac{1}{\rho}\left\{p_{\rm h} + \frac{2\sigma}{r} + \frac{4\mu\dot{r}}{r} - (p_{\rm g} + p_{\rm v})\right\} - \frac{p_{\rm M} R_{\rm ch} k \sin\omega t}{\rho}$$
$$\times \left\{1 - \exp\left(-\beta\left|\frac{r\omega}{\sqrt{3\gamma(p_{\rm g} + p_{\rm v})/\rho}} - 1\right|\right)\right.$$
$$\left. + \frac{1}{kr}\exp\left(-\beta\left|\frac{r\omega}{\sqrt{3\gamma(p_{\rm g} + p_{\rm v})/\rho}} - 1\right|\right)\right\} = 0\,. \qquad (35)$$

Numerically integrating Eqn (35), we found that the sound pressure $p'_{\rm a} = p_{\rm M} R_{\rm ch} k$ is exerted on the bubble throughout its motion, but at the moment when the bubble size is near the resonant one the sound pressure sharply increases and ranges up to 100 – 1000 atm once or twice during the period of acoustic vibrations. According to the calculations by the new dynamic equations for the solitary cavitation bubble [145], which take into account the focusing, the dependence of the acoustic energy absorption on the bubble radius (35), and the liquid vapor pressures by Eqns (4) and (6), we found that the maximum theoretical radius is $R_{\rm m} \approx 86$ μm (Fig. 7), and the latter value is sufficiently close to that obtained experimentally by Crum [13] ≈ 80 μm, and by Barber and Putterman [11] ~ 70 μm (Fig. 8). The calculated maximum velocity of travel of the wall for a solitary cavitation bubble is 1400 m s^{-1} (Fig. 7e) and close to the experimental maximum velocity 1300 m s^{-1} recorded in Ref. [11]. The absorption coefficient reaches a maximum value $G(r) \sim 1$ twice during the period of acoustic vibrations (Fig. 7b).

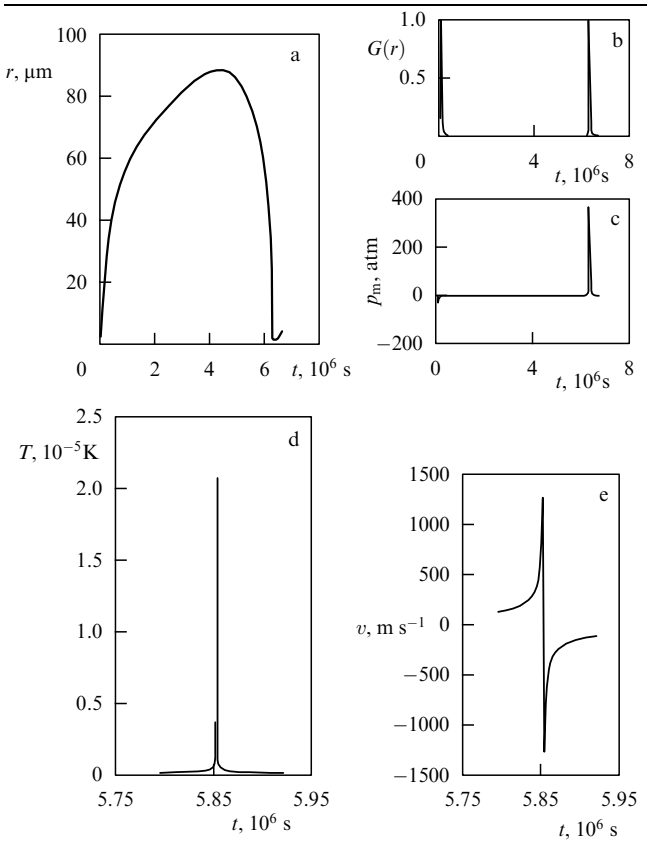

Figure 7. Time dependences of the radius of a solitary air cavitation bubble in water (a), that of the absorption coefficient (b), that of the pressure in the liquid on the bubble surface (c), the temperature in the cavitation bubble (d), and the velocity of the bubble wall travel (e) calculated by (35) and with an account for the vapor pressure using (4) and (6) [145]; the field parameters are the following: $f = 26$ kHz, the pressure on the chamber surface is $p_{\rm M} = 1.0/\pi = 0.31$ atm, and $r_0 = 2$ μm.

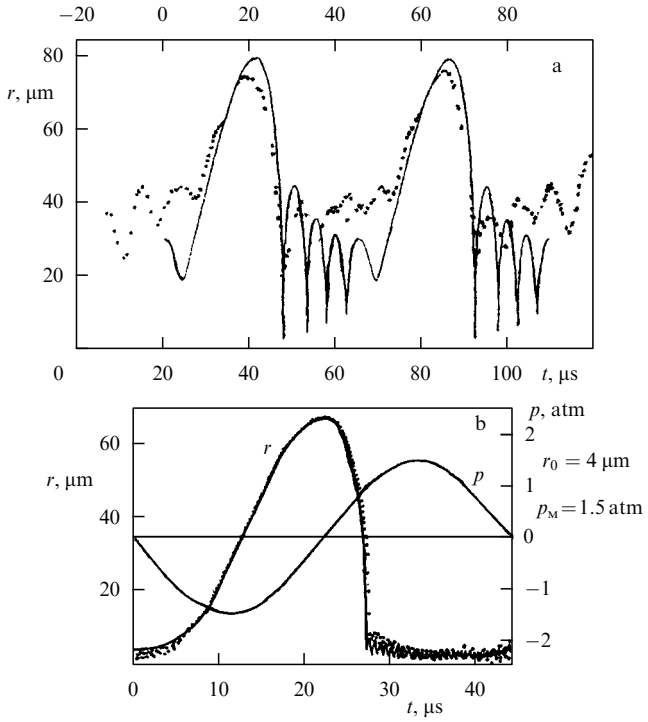

Figure 8. Experimental (dots) and theoretical (lines) time dependences of the radius of a solitary cavitation bubble [13] (a) and [11] (b).

However, we should exclude bubbles of very small size from the consideration, since formula (33) can be applied in the approximation when the cavitation bubble radius exceeds the thickness of a thermodiffusive layer in liquid, which is equal to 11 μm in water at $T_\infty = 20\,^\circ$C [184]. When the sound pressure is higher, we should take into account the compressibility of liquids and numerically integrate the Keller – Miksis equations together with relations (31) and (34). The theoretical dependence $r(t)$ calculated in Ref. [145] (Fig. 9) fully coincides with the experimental data [11]. Accounting for the compressibility of liquids results in a maximum velocity of the bubble wall travel of about 2.3 km s^{-1}. In the liquid phase, the minimum sound pressure occurs for the bubble expansion, and the maximum one for the bubble compression, the latter ranging up to 100 – 1000 atm due to the focusing effect (Figs 7c and 9d). The maximum temperature is about $(2-3) \times 10^5$ K and occurs for the maximum compression of the cavitation bubble (Figs 7d and 9f).

The data obtained in Ref. [145] allow us to propose that something like an acoustic 'black hole' arises at the center of a single-bubble chamber in originating a single-bubble SL, which has dimensions much shorter than the sound wavelength but absorbs a substantial portion of the acoustic energy during a short time. In this case the main 'shock' of the acoustic field takes place once or twice during the period, depending on the resonant radius (for this absorption the size

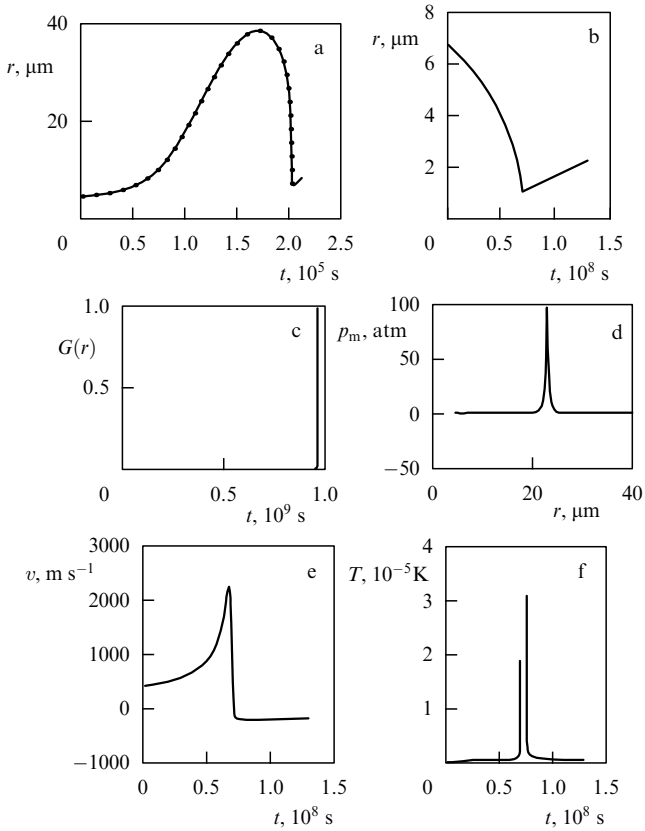

Figure 9. Time dependences (a) (dots mark experimental and theoretical findings from Ref. [11]) and (b) of the radius $r(t)$ of a solitary air cavitation bubble in water, (c) that of the absorption coefficient $G(r)$, (d) the pressure $p_m(r)$ in liquid at the bubble surface calculated by (35) as a function of the bubble radius, (e) that of the velocity v of the bubble wall, and (f) time dependence of the bubble temperature. The time dependence of the radius $r(t)$ is calculated using (31), (34) and the Keller – Miksis equation. The vapor pressure is accounted using (4) and (6) [145]. In contrast to the data depicted in Fig. 8, the above data take into account the compressibility of liquids and the fact that formula (33) can be applied only when $r > 15$ μm [184]. The parameters of the field are the following: $f = 26.5$ kHz, the pressure on the chamber surface $p_M = 1.325/\pi = 0.42$ atm, and $r_0 = 4.5$ μm. All features on the curves (a) – (f) correspond to the point of the maximal compression.

of the 'black hole' should be comparable with the bubble resonant radius rather than with the sound wavelength). The supposed theory also explains similar effects arising in the cylindrical resonator, where two or more solitary cavitation bubbles are sometimes observed on the axis of a focusing unit [163] at distances exceeding the separation at which they can effectively interact. According to Ref. [145], we believe that at least two conditions are required to be fulfilled for producing single-bubble SL, namely, to generate a focused harmonic acoustic wave and to provide the stable spherical shape of the cavitation bubble. Introduction of additional cavitation bubbles which can interact with the pulsating solitary cavitation bubble or another elements breaking the symmetry interrupt the light emission accompanying single-bubble SL.

Thus, we proposed in Ref. [145] the mechanism of effective concentration of the acoustic energy, which enable us to achieve with theoretical approach based on novel dynamic bubble equations the high values of the parameters T_{max} and $\dot{r}_{max}$ inside the cavitation bubble even accounting for the real value of vapor pressure in the bubble at sound pressure amplitude ~ 1 atm. These results allowed us to explain the difference in behavior of the single- and multibubble cavitation and hence SL effects. In addition, we can also explain the origin of high values of maximum temperature, pressure, and velocity of the bubble wall travel and, hence, the arising high-temperature glow, bremsstrahlung, shock waves, etc. in the process of single-bubble cavitation for $p_M \sim 1$ atm.

We believe that in future the acoustic bubble chamber will be improved and it will be possible to develop an installation in which even thermonuclear temperatures will be achieved inside solitary cavitation bubble due to the high-energy concentration and the occurrence of thermonuclear reactions D + T [9, 95, 100, 101, 124, 140]. To our opinion the compression of a gas target by sound pressure could be more convenient than by laser radiation [146]. We do not exclude also the possible combination of these effects. Although ultrasound physics and its applications have been developed over a time period thrice exceeding that for laser physics, their modern states and rates of advance can hardly be compared. Thus, new fields of scientific and industrial applications may undoubtedly promote the progress in acoustics and related areas of science.

5.6 Shock waves in the cavitation field

The hypothesis that shock waves and, accordingly, high local temperatures arise in collapsing cavitation bubbles, even though there is only a solitary bubble, has been considered by many researchers. The authors of Refs [58, 59] recorded shock waves in fluid for multibubble cavitation by the holographic technique and showed that these effects usually accompany the collapse of cavitation bubbles. Shock waves are often events in multibubble cavitation under the action of high sound pressures. In Ref. [137], the velocities of expansion and compression of a solitary cavitation bubble were studied by the laser interferometry method, which yielded the measured maximum velocity of the bubble wall travel under compression to be 350 m s^{-1}, the accuracy of measurements being 20%. Barber and his colleagues [11] used a maximum intensity of ultrasound (1.45 W cm^{-2}) on the single-bubble chamber surface and estimated the velocity $\dot{r}_{max}$ of a solitary cavitation bubble compression at the final stage to be about 1300 m s^{-1}. It should be pointed out that in general case the shock waves can be set up in a cavitation field by either of two mechanisms:

(1) A shock wave occurs in the liquid due to high pressures at the bubble – liquid boundary, when the bubble compression is maximum. However, this shock wave cannot generally account for intense SL, since it propagates through the liquid and not in the bubble.

(2) When the cavitation bubble collapses, a shock wave arises inside the bubble and propagates to the bubble center.

In the studies of multibubble cavitation, most often consideration has been given to the first mechanism [148], since up to now no reliable experimental methods for measuring the velocity of the bubble wall travel in multibubble cavitation field have been developed. Numerical calculations made in Ref. [149] demonstrated that when the maximum pressure p_{max} inside the bubble exceeds 10^3 atm, the ratio between the distance at which the shock wave is formed and the minimum bubble radius is about 5 – 6. At low sound pressures, an acoustic wave of finite amplitude moving away from the bubble is weak, and the distance between the bubble center and the point on the surface where the wave

forms is rather large. Calculations using conventional equations for the dynamics of cavitation showed that a shock wave does not arise generally at 1–2 atm and $p_{ad} \geqslant 2 \times 10^{-2}$ atm, which are typical of the single-bubble SL formation. Actually, for adiabatic compression of the bubble, it follows from Eqns (10) and (11) that

$$p_{max} \approx p_{ad} \left(\frac{p_h + \langle p_M \rangle}{p_{ad}} (\gamma - 1) \right)^{\gamma/(\gamma-1)},$$

where p_{ad} is determined by Eqn (6), p_{max} decreasing with increasing γ. According to NN Eqn (5), the maximum pressure $p_{max} \sim 10^3$ atm should be observed in a compressed bubble even at moderate sound pressures. However, a correct account of the vapor pressure dependence on the bubble radius at its compression [see Eqn (6)] results in $p_{ad} = p_{g\,min} + p_s > p_s$, and the value of p_{max} appears considerably less. Accounting only for heat conductivity also decreases p_{max} by an order of magnitude [147]. Numerical estimates showed that in the case of multibubble cavitation a pressure exceeding 10^3 atm can be attained inside a compressed cavitation bubble only when the sound pressure is higher than 10–15 atm, which is in agreement with the experimental data [57, 59].

Rather intense shock waves were recorded in the case of single-bubble cavitation [11], thus within ~ 1 mm of the bubble the amplitude of the shock wave was 3 atm. In these experiments the building-up time during which the pulse increased was limited by the resolution of the hydrophone (up to ~ 10 ns), the fall time during which the pulse decreased was about 30 ns. At $r_{max} = 0.5$ μm, the intensity of the shock wave on the bubble surface was about 6000 atm [11] even when absorption was lacking [11]. But in practice, a shock wave is absorbed rather intensively, for example, for a 300-MHz harmonic wave the pressure pulse decreases approximately 10^4-fold at a distance of 1 mm [11].

The second mechanism implies the formation of a shock wave inside the cavitation bubble. The hypothesis for the formation of shock waves inside a solitary cavitation bubble and a local increase in the temperature of steam–gas mixture at the same site is held by many researchers, since it explains the rather short duration of SL pulses, the problem being solved very naturally by the time of light emission from the most compressed region of the shock wave [124, 128, 151, 154]. The shock wave is naturally proposed to originate when the velocity of the bubble wall travel exceeds the velocity of sound in gas, and then the intense converging spherical shock wave is treated by the approximate Guderley equation [174]. However, some points need to be made regarding this model.

(1) At the initial moment, the maximum velocity of the bubble wall travel at 1-atm sound pressure is less than the velocity of sound in gas, and even less than the sound speed c_g in the compressing bubble (since $c_g \sim T^{1/2} \sim r^{-3(\gamma-1)/2}$ and for $\gamma = 4/3$ one finds $c_g \sim r^{-1/2}$). Actually, assuming the gas in the bubble to be ideal and ignoring its viscosity and surface tension (which decreases the maximum velocity) we find from Eqn (13) that

$$\dot{r}^2_{max} \approx \frac{2p_{ad}}{3\rho} \left(\frac{A}{\gamma} \right)^{\gamma/(\gamma-1)} \xrightarrow{\gamma=4/3} \frac{2p_{ad}}{3\rho} \left(\frac{p_h + \langle p_M \rangle}{4p_{ad}} \right)^4.$$

The increase of γ up to 5/3 decreases the power index from 4 down to 2.5 and substantially reduces the maximum velocity. Under normal conditions for water ($T_0 = 300$ K, $p_v = 0.0025$ atm), for sound pressure $p_M = 1.325$ atm (at adiabatic compression $\langle p_M \rangle \lesssim 0.3$ atm), and hydrostatic pressure $p_h = 1$ atm, we obtain $\dot{r}_{max} \approx 218$ m s^{-1}. Accounting for only the heat conductivity decreases this value twice or more [147]. Additional consideration of viscosity, nonideal behavior of steam–gas mixture, etc. yields a maximum velocity of the bubble wall travel to be less than 100 m s^{-1} at the pressure of $p_M = 1.3$ atm in the case of multibubble cavitation.

(2) We should also take into account that a certain path is required for a shock wave to be formed. At this path the front of the finite-amplitude wave is 'turned over' and the shock wave thickness makes up several mean free paths. Therefore, the shock wave in the motion of the disturbance directed to the bubble center may not manage to be formed (at least, this point requires special consideration).

Using the new dynamic equation (35) for a solitary cavitation bubble allow us to obtain by calculations a velocity of the bubble wall travel which is about 1300 m s^{-1} or more [145]. Thus, the probability of formation of shock waves inside a solitary cavitation bubble is high and this problem becomes topical.

6. General analysis of experimental and theoretical data

6.1 Mechanism of multibubble SL

In paper [112] we determined the main energy parameters of SL flashes produced by multibubble systems in the ultrasound field at the frequency of 20 kHz:

(1) the total number of pulses is $N \approx 2.5 \times 10^5$ per second;
(2) the average energy of the pulse is $\langle E \rangle \sim 3.3 \times 10^4$ eV;
(3) the energy of an intense pulse is $E_{max} \sim 1.3 \times 10^5$ eV;
(4) the acousto-optic efficiency is $\eta_{ao} \sim 4.4 \times 10^{-11}$;
(5) flashes with energies in the range 1.3×10^4–1.3×10^5 eV emit 70% of the total SL luminous flux;
(6) the duration of the SL pulse is 3 ns at the intensity $U/2$.

The thermal theory and the theory of local charging seem to be the most well-developed and substantiated to explain the mechanism of origination of multibubble SL. The first of the fundamental problems in this area is to reveal whether SL produced in multibubble cavitation fields has a thermal or electrical origin. Table 1 lists the main experimental data and their correspondence to these two theories.

Thermal theories can hardly explain initiation of multibubble SL and sonochemical reactions at low ultrasound intensities (about 10^{-3} W cm^{-2}), at high liquid temperatures $T_\infty \sim T_{boil}$, at decreased hydrostatic pressures when the difference $p_h - p_v$ is small, and for high medium viscosity. When $T_\infty \sim T_{boil}$ and $p_h \sim p_v$, the cavitation bubbles cannot collapse because more likely they grow. At very low ultrasound intensities and extremely high medium viscosities, the pulsations of bubbles turn out to be negligible and the bubble cannot collapse even theoretically. Figure 10 plots a semilogarithmic dependence of the maximum increase in temperature ΔT_{max} in a cavitation bubble against the amplitude of sound pressure and fluid viscosity calculated even by the modified RP equation (9)[7]. The shaded region

[7] The modified RP equation yields an overestimated value for ΔT_{max}, since it cannot take into account many effects decreasing the temperature in a collapsing cavitation bubble such as: heat-and-mass transfer, compressibility of liquids, the interaction between neighboring pulsating bubbles, the deformation of cavitation bubbles, etc.

Table 1. Experimental facts and their correspondence to the thermal and local charging theories of a cavitation bubble in multibubble SL [9]*.

Experimental facts	Thermal theories	Theory of local charging	References
(1) The maximum probability of SL pulse at $\langle r\rangle \sim 0.8\langle R_{\max}\rangle$	–	+	[31]
(2) SL and sonochemical reactions at $f \sim 100$ Hz; absence of cavitation bubble collapse	–	+	[32, 77, 102]
(3) Substantial difference between the SL spectra and the continuum of blackbody radiation	–	+	[41 – 44, 52, 53]
(4) Fast decrease in the intensity of the Na D-line as the time gap between ultrasound pulses increases	–	+	[9, 28]
(5) SL at $T_\infty \sim T_{\text{boil}}$ and $p_{\text{h}} \sim p_{\text{v}}$	–	+	[25]
(6) SL for fast evacuation of the chamber	–	+	[8, 9]
(7) SL in dc electric field and on electrolysis	±	+	[103, 104]
(8) Electrical pulses in a cavitation field	±	+	[105]
(9) Ultrasound glow in mercury and metal melts	–	+	[8, 18, 19]
(10) SL in liquids and polymers with a high viscosity at the onset of their melting	–	+	[8, 9]
(11) SL and sonochemical reactions at low ultrasound intensities (about 10^{-3} W cm^{-2})	–	+	[87]
(12) Absence of H_2O_2 formation and synthesis of NO in pulsed units of adiabatic compression; formation of H_2O_2 and NO on electrical discharges in water	–	+	[108, 107]
(13) Random time for generation of SL pulses	–	+	[31]
(14) SL flashes in phase when $\langle r\rangle = 0.8R_{\max}$	–	+	[176]
(15) SL quenching; linear dependence of the quenching efficiency U/U_{q} on the impurity concentration	–	+	[4, 8, 44, 109]
(16) Dependence of U/U_{q} on the structure of quencher; increase in U/U_{q} as the boiling temperature T_{boil} of the quencher increases	–	+	The same
(17) Increase in the efficiency of the suppression of the sonochemical reaction rate for rising T_{boil} of an additive	–	+	[9, 110]
(18) SL is a luminescent cold emission based on items 15 – 17	–	+	[111]

* The symbol + stands for the agreement with the theory; – means inconsistency, and ± signifies that a conformity between the theory and experiment can hardly be established.

corresponds to the experimental conditions under which SL and sonochemical reactions occur [9].

According to the data presented in Table 1 and Fig. 10, the thermal theories accounting for the origin of SL and other high-energy effects in ordinary multibubble cavitation fields are valid only for a narrow range of experimental conditions (the ABC triangle in Fig. 10). Under other experimental conditions, the thermal theory and its modifications are inadequate, since they cannot explain the generation of SL at temperatures higher than ~ 2000 K. The conditions for the occurrence of SL in a single-bubble system fall into the *ABC* region in Fig. 10.

Items 15 – 18 in Table 1 should be clarified. The studies [44, 109] on the influence of additives on SL in water revealed the dependences:

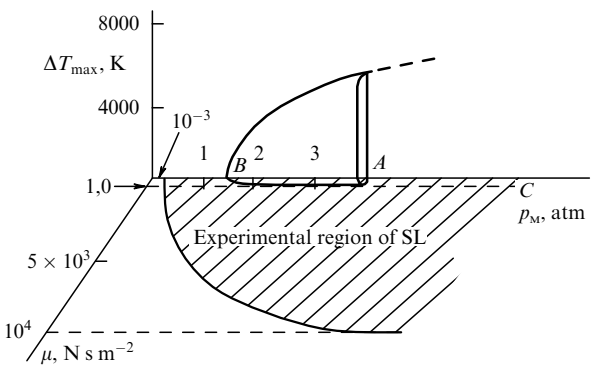

Figure 10. Dependence of the maximum increase in the temperature inside the cavitation bubble on the amplitude of sound pressure [calculated by the modified RP equation (9)]; the shaded region corresponds to the experimental conditions at which SL and sonochemical reactions occur [9].

— the influence decreases along the series: benzene > t-butanol > n-propanol > ethanol > methanol > potassium iodide > α-naphthol (the latter two additives quench SL in liquids);

— the influence of additives on sonochemical reactions decreases in a similar way [110].

The influence of additives cannot be explained in the framework of an approach preventing bubble collapse as the thermal theory would suggest, since the additives with enhanced T_{boil}, such as butanol, should penetrate the cavitation bubble with a lower probability than, for example, methanol does and decrease U to a lesser extent. To explain the experimental data, some other suggestions are required, namely, that U is decreased by additives due to quenching of excited M* states by molecules of a quencher S in the gas phase:

$$\text{M}^* + \text{S} \longrightarrow \text{M} + \text{S} + q\,.$$

An additive proves to be a more effective quencher not due to its low T_{boil}, but owing to an increased number of molecular vibrational levels over which the M* excitation energy dissipates. Thus, for instance, alcohols with a long molecular chain are more effective quenchers of SL in the gas phase, though their concentration is small. The excitation energy can be unilaterally transformed into heat only when the substance and the radiation are not in temperature equilibrium and therefore, according to the above reaction, the quenching by the collisions of the second kind cannot occur in the presence of blackbody radiation. If this were the case, the quenching molecules would penetrate the growing cavitation bubble, assume the bubble temperature and radiate at the moment of bubble collapse as does the steam – gas mixture in the bubble. The possibility of quenching SL by Frank – Hertz collisions of the second kind gives evidence in favor of the nonequilibrium

luminescent nature of light emission and suggests that *in the course of multibubble SL the cavitation bubbles should be cold* [111].

Thus, the only theory that is consistent with most of the currently available experimental data on multibubble cavitation fields is the theory of local charging of cavitation bubbles [74, 81, 83, 85, 153].

6.2 Mechanism of single-bubble SL

It should be pointed out that apart from the thermal theory accounting for the origin of single-bubble SL, sonochemical reactions, and other high-energy processes in cavitation fields, there are also some other models, but at present they are not competitive with the thermal approach to the SL occurrence. Let us consider some of them.

The authors of Refs [113–115] advanced a fundamentally new and interesting hypothesis which proposes that the light emission accompanying the motion of the cavitation bubble wall to vacuum results from the dynamic Kasimir effect (the theory of quantum vacuum radiation). Eberlein [114, 115] obtained the following formula for the sono-induced flash energy:

$$E_c = 2.4 \times 10^{-3} \frac{(n^2-1)^2}{\pi n^2} \int_0^{T_0} \frac{\partial^5 r^2(\tau)}{\partial \tau^5}\, \dot{r}(\tau) r(\tau)\, d\tau\,, \qquad (36)$$

where n is the refractive index of the liquid, and T_0 is the period of acoustic vibrations. Taking into account that $\dot{r} \sim (r_0 - r_{min})/t_c$[8], Eberlein [114] obtained the formula for E_c:

$$E_c = 6.8 \times 10^{-3} \frac{(n^2-1)^2}{n^2} \frac{\hbar}{c^4 t_c^5} (r_0^2 - r_{min}^2)^2\,, \qquad (37)$$

where c is the speed of light. Even assuming that the cavitation bubble collapses starting from its maximum radius, we obtain an energy of the SL flash approximating the experimental value, $E_c \sim 2.5 \times 10^{-16}$ J[9], only when the duration of the SL flash is $t_c \sim 1$ fs [115], which corresponds to a supraluminal speed of bubble wall travel of about $\dot{r} \sim 30c$ (!), and has no physical meaning. Note that Eberlein [114, 115] did not find any relations between the physical parameters inside the cavitation bubble, obtained under various experimental conditions, and the peculiarities of the conjectured SL emission. According to Ref. [116], the intensity of quantum vacuum radiation must be many orders of magnitude lower than the energy of the ordinary ultrasonic SL and, besides, it must not vary sharply as the composition of gas phase changes slightly, for example, due to very low additions of inert gas.

Garcia and Levanyuk [117] considered the mechanism of quantum vacuum radiation, proposed in Ref. [114]. Each elementary process of radiation corresponds to the emission of a pair of photons ω, ω' with the energy $\hbar(\omega + \omega') = \hbar\Omega$, where Ω is the frequency of light. According to the theory [114, 115], the number of photons radiated during one SL flash is equal to

$$N_a = \alpha \int_0^{\infty} \left(\int_0^{T_0} d\tau \frac{r^2(\tau)}{c^2} \exp(i\Omega\tau) \right)^2 \Omega^5\, d\Omega\,, \qquad (38)$$

where $\alpha \sim 10^{-4}$ is the numerical coefficient for the air–water interface. The calculations yield

$$N_a = \frac{15\pi^2}{16} \alpha \left(\frac{r_0^2 - r_{min}^2}{c^2 t_c^2} \right)^2 . \qquad (39)$$

The characteristic time of bubble collapse $t_c \ll T_0$ is short and even at the maximum velocity of collapsing $\dot{r}_{max} \sim 1$ km s^{-1} the number of photons N_a emitted during one SL flash cannot exceed 10^{-23} (which corresponds to one-photon emission every 10^{11} years). But the experimental value of $N_a \sim 10^5$ differs from the theoretical estimate by 28 (!) orders of magnitude. A similar difference of 25–26 orders of magnitude exists between the experimental and theoretical estimates of the sonoflash energy obtained in Ref. [117]. The authors of Ref. [118] calculated the energy efficiency of the sonoflash caused by the vacuum quantum radiation, taking into account the fifth time derivative of the cavitation bubble radius:

$$E_c = N_a \int_0^{T_0} \frac{\partial^5 r^2(\tau)}{\partial \tau^5}\, \dot{r}(\tau) r(\tau)\, d\tau\,, \qquad (40)$$

and found the energy of one SL flash to be about $E_c = 3 \times 10^{-48}$ J. Numerical integration of $r(t)$ yielded still less energy $E_c = 2.5 \times 10^{-55}$ J. At the same time, the experimental value of an SL flash energy is $E_c \sim 5 \times 10^{-14}$ J for single-bubble SL [11], and $\sim 5 \times 10^{-15}$ J for multibubble one [112]. Therefore, the theory of quantum vacuum radiation, if it proves viable at all, calls for substantial improvement.

Mohanty and Khare [119] proposed a new model where SL origin is treated as a result of a cooperative interaction between particles inside a cavitation bubble and the emitting field. This interaction can be divided into two stages. At the first stage, the bubble compresses thus enhancing the number density of excited atoms and molecules. Frommhold and Atchley [120] considered SL as light emission caused by collisions. Upon compression, the bubble reduces to a minimum size, the temperature and pressure inside it rise, and the gas becomes highly excited or ionized. Excited atoms can return to the initial state by spontaneous emission. According to Ref. [119], if the distance between excited particles is less than a characteristic length corresponding to the wavelength of emitted light, the phases of electromagnetic radiation should be correlated. The total radiation field of N_a atoms is a superposition of fields of individual atoms:

$$E_c = \Sigma E_i \sim N_a\,, \qquad (41)$$

while the intensity of emitted light is $U \sim E_c^2 \sim N_a^2$. For ordinary radiative deactivation we have $U \sim N_a$. But in the case of co-operative spontaneous radiation, which is the second step of light emission, one finds

$$U \sim N_a^2\,. \qquad (42)$$

The hypothesis offered in Ref [119] allows a prediction that the emitted light is coherent, which can be detected experimentally. At the same time, the model is still not sufficiently advanced and it is hidden from view how it can explain many other experimental facts.

Prosperetti [121] proposed a hypothesis that the liquid near the surface of an expanding cavitation bubble cools considerably to form a thin ice layer at the bubble surface.

[8] Using this relation overestimates the energy of an SL flash, since a single bubble starts collapsing when its radius is less than the maximum radius r_{max}.

[9] In fact, the value of E_{sf} may be at least two orders of magnitude higher [112].

The breaking of this ice in water produces SL. Although this hypothesis has not been perfectly developed as yet, one can make some essential comments:

— SL is observed not only in water, but in some other liquids such as ethanol [129], whose freezing temperature is $-114\,^{\circ}$C, but this low temperature cannot be attained at moderate ultrasound intensities;

— the light should be emitted at $r \sim R_{\max}$ until the ice layer is molten, but this contradicts the experimental data;

— in the general case, the SL emission spectra should differ from those obtained in ice breaking.

— Lepoint et al. [51, 122] hypothesized that a fluid jet breaking up into microdrops is formed inside the cavitation bubble. Due to the Lenard effect the drops should acquire a charge. In principle, this hypothesis cannot be applied to single-bubble systems, since no jets have been detected there by different optical methods. For multibubble SL this model is inadequate for many reasons, the main of which are:

— at a frequency of, for example, 1 MHz, the cavitation bubble radius is $\sim 5 \times 10^{-7}$ m, $r_{\min} \sim 5 \times 10^{-8}$ m and a jet with microdrops can hardly be held inside a compressed bubble, and all the more neither can the dense and diffusive portions of the double layer hold inside a jet of radius 3×10^{-9} m, bearing in mind that the kinetic diameter of the water molecule is $\sim 5 \times 10^{-10}$ m;

— no fluid jets directed to the cavitation bubble center have been recorded to arise at the moment of the bubble collapse in a bulk liquid, while cumulative jets directed to the solid surface have been detected and well studied [68];

— when the pressure inside the cavitation bubble is thousands of atmospheres, there are not any reasons for the formation of the thin jet and microdrops directed to the bubble center.

The analysis of experimental and theoretical studies of SL leads us to conclude that the most probable mechanism of single-bubble SL is the thermal one. At present we can indicate the main modifications of the thermal theory of sonoluminescence:

— the blackbody emission, which was carefully considered above;

— bremsstrahlung caused by ionization of the steam – gas mixture inside the cavitation bubble [123 – 125,180];

— the hypothesis of the generation of shock waves inside the cavitation bubble, the main ideas of which were put forward in Refs [57, 123] and developed more fully in Refs [127, 128] and other works.

Gompf and his colleagues [125] improved the procedure for determining the duration t_c of SL flashes. In contrast to the previous works, they used light filters transparent to radiation with wavelengths of 300 – 400 and 590 – 650 nm, which were maintained before the photomultiplier to record SL flashes. This enabled them to detect the duration of the ultraviolet and red portions of the spectra of single-bubble SL pulses. According to their results [125], the durations of these spectral portions are the same within the accuracy of experimental investigations. Treating the single-bubble SL as equilibrium blackbody radiation, they naturally explained the duration of the ultraviolet portion of an SL pulse, the increase in the total duration of an SL pulse with growing sound pressure and concentration of dissolved gas, and the enhancement of the total radiation energy. However, for thermal radiation of a black body, the duration of the red portion of the SL pulse should be longer than that of the ultraviolet one.

If we assume that the SL is bremsstrahlung, the similar durations of the red and ultraviolet portions are explained quite naturally [125, 180]. However, this reason cannot explain the total energy of an SL pulse. Since the intensity of bremsstrahlung is proportional to the square of acceleration of a charged particle, and the acceleration is inversely proportional to the mass of the particle, the bremsstrahlung of electrons should be millions of times more intense than the radiation of protons, and still much higher than that of ions. The bremsstrahlung spectrum of electrons is continuous and limited by the maximum energy of photons corresponding to the electron energy. The bremsstrahlung is mainly effected by the electrons whose energy E is higher than $E_{\rm cr}$; at $E < E_{\rm cr}$ most of the energy is supplied to excitation and ionization of atoms. Bremsstrahlung can be rather intense for thermal motion of particles in hot rarefied plasma at temperatures higher than $10^5 - 10^6$ K and is dominant when the energy of electrons is rather high. For temperatures of 50 000 – 100 000 K and low density of the medium, bremsstrahlung can contribute to the total emission, but in any case it is only a part of the radiation, which also involves the (thermal) blackbody radiation. If the duration of a pulse induced by bremsstrahlung is shorter than the duration of a pulse caused by thermal emission, the dependence of the SL pulse duration t_c on the wavelength λ should be similar to the dependence $T(\lambda)$ for the blackbody radiation. Another possibility is not excluded: the duration of the bremsstrahlung pulses is somewhat longer than that of the blackbody radiation. So, while the thermal radiation is dominant in energy, the duration of the light pulse is determined by the duration of the bremsstrahlung pulse. Obtaining evidence in favor of a considerable contribution of bremsstrahlung to the single-bubble SL emission may enable one to determine more precisely the high temperature in a collapsing solitary cavitation bubble; in this case it must approach to the maximum temperatures considered in Section 5.5.

According to Yasui [180], single-bubble SL results from adiabatic compression of the cavitation bubble. It has a thermal origin, but presents a bremsstrahlung caused by interaction between an electron and atom or ion rather than the thermal emission of the black body. However, the bremsstrahlung is considered in Ref. [180] at 10 000 K, and under these conditions the intensity of bremsstrahlung is very low. Application of equation (35) for the dynamics of a solitary cavitation bubble in accordance with the theory [145] leads to high values of parameters for the cavitation bubble and, accordingly, requires an account of bremsstrahlung.

Let us consider the plasma peculiarities for ultrashort-duration single-bubble SL pulses and, accordingly, the short lifetime of plasma inside the cavitation bubble. At a temperature of about $\sim 10^5$ K, the steam – gas mixture inside the bubble is fast ionized and dissociates (see Section 5.5) and the plasma produced is considered equilibrium. The value of the Debye shielding radius in the plasma at the maximum compression is given by the formula

$$d_{\rm sh} = \sqrt{\frac{kT_{\max}}{8\pi e^2 n_e}}\,,$$

where n_e is the number density of electrons, and e is the electron charge. At $T_{\max} = 10^5$ K and $n_e = 10^{21}$ cm^{-3}, we have $d_{\rm sh} \sim 10$ A $\ll r_m$, Thus, the plasma inside the bubble is quasi-neutral, and ambipolar diffusion takes place. In other

words, electrons diffuse towards the bubble wall together with ions, the diffusion coefficient being equal to $2D_i$, where D_i is the diffusion coefficient for ions.

If single-bubble SL is caused by the thermal mechanism alone and the blackbody emission is observed then, in principle, there should not be any difference in the emission spectra of the bubbles containing various gases (a variation in the emission intensity can only be due to different physicochemical parameters of the gases, which come into importance only at the stage of bubble compression). The spectrum of bubbles not containing noble gases is similar to that of a black body [89]. As for the bubbles containing He, Ne, and Ar, their spectra, conceptually, can be treated as emission of a black body, but for Xe and Kr they have a broad maximum at ~ 300 nm [11]. To explain so substantial difference in the single-bubble SL spectra, we should consider not only equilibrium mechanisms, but also nonequilibrium effects leading to luminescent emission. Therefore, we may believe that single-bubble SL can partly result from a luminescent deactivation of excited atoms, at least of Xe^* and Kr^*, which can be produced by recombination of ions and electrons upon cooling of the cavitation bubble. In this case, the total duration of an SL pulse should exceed 0.35 ns, which is the duration obtained for solitary cavitation bubbles containing O_2 or N_2 [125]. This viewpoint provides a quite natural explanation for two-orders-of-magnitude more intense emission of cavitation bubbles filled with inert gas. The spectrum of an SL flash can have then an intricate shape with two maxima, the second one being greater.

In the spectrum of single-bubble SL, the emission intensity depends on the wavelength as $\lambda^{-2.5}$ [134]. In the case of quantum vacuum radiation [114, 115], this dependence would be different: λ^{-3}. For thermal emission of a black body we would have λ^{-4} (according to the Planck law), and for bremsstrahlung — λ^{-2} [139]. One would expect in the case of bremsstrahlung combined with the blackbody emission that this dependence is proportional to $\lambda^{-2.5}$. This 'two-component model' of single-bubble SL is held by Tsiklauri [175].

Chou and Blackman [135] found a difference in SL spectra obtained at different scattering angles, which is due to nonuniform distribution of electrons in strong magnetic fields. Young and his collaborators [101] applied a strong magnetic field when studying single-bubble SL[10] and discovered a range of effects. They observed that the SL flux decreases as the field intensity rises up to 20 T. Besides, at 20 °C, the stability region of a solitary cavitation bubble in a magnetic field expands and at increased sound pressure the maximum SL intensity enhances. Yasui [181] proposed that the dynamics of single cavitation bubbles changes in a strong magnetic field due to the action of the Lorentz force on electric dipole moments of water molecules, resulting in a partial transformation of their kinetic energy into heat. The reason for these effects is still unclear. In our opinion, the electrons and, to a lesser extent, ions which are produced in abundance as a result of multiple ionization of atoms and molecules in the cavitation bubble, can move (under the special conditions of the experiment) along rounded trajectories under the action of a strong magnetic field and, hence, the field can stabilize their motion. This extends the stability region for a solitary cavitation bubble and enhances the SL emission. We also do not exclude the possibility that deformations can develop at some stages of the motion of a solitary cavitation bubble (for example, near the phase of its maximum compression) and they occur not only in multibubble systems but in a solitary cavitation bubble as well. Under certain conditions electrical processes take on significance and the influence of a magnetic field may be appreciable.

[10] The authors of Ref. [101] nowhere indicated what type of SL they studied, however, taking into account some details of the experiment we think that they consider single-bubble SL.

7. Conclusions

Until recently the thermal theory of multibubble cavitation proposed by Noltingk and Neppiras (1950) was held by most researchers. It was all the more natural in view of the fact that the electric theory proposed by Frenkel' in 1940, proved inadequate. The theory of local charging of a cavitation bubble, developed by Margulis (1985, 1997), allowed the substantiation of the electrical mechanism of origin of high-energy effects in ultrasound fields, which fits most of the experimental data. We may think of the following sequence of processes occurring in a pulsating bubble. The bubble radius increases due to the absorption of gas dissolved in liquid until it approaches the resonant radius, then the bubble is deformed, loses its stability and fragments. Local uncompensated electric charges arise upon the bubble splitting and deformation and the local electric field strength can exceed the critical one. Electric discharges are accompanied by excitation and decomposition of molecules of steam – gas mixture inside the cavitation bubble and, accordingly, by SL emission and sonochemical reactions in cavitation fields.

The discovery of single-bubble SL by Crum (1991) showed that for a certain configuration of an acoustic field a stably pulsating solitary bubble arises which strongly differs from 'ordinary' cavitation bubbles. Further experiments revealed that the essential difference between single- and multibubble cavitation is governed by two main reasons: (i) the energy of the acoustic field is far more effectively concentrated as a result of the focusing effect and (ii) increasing the fraction of absorbed acoustic energy by a solitary bubble, which is described by the parameter $G(r)$ entering Eqn (31); one possible explanation of this effect calls for the enhancement of ultrasound absorption by a cavitation bubble on its approaching the resonance size. The equations for the dynamics of a solitary cavitation bubble in the field of a spherical harmonic acoustic wave were obtained with due regard to the most important factors such as focusing of the acoustic field, nonideal effects for gas, different dependences of the partial liquid vapor pressure in the phases of expansion and compression of the cavitation bubble, and partial absorption of the sound wave energy by the bubble. These equations differ from the ordinary dynamic equations for cavitation.

The proposed theory provides an explanation for the single-bubble SL effect and the conditions under which it arises. Due to the symmetry of the acoustic field, a solitary cavitation bubble is not practically deformed, neither does it fragment and hence no local charging of the cavitation bubble can occur. Therefore, solitary pulsating bubble SL has a thermal origin different from the cold luminescent emission of an ensemble of cavitation bubbles, caused by charging effects in the case of multibubble SL. The independence of the duration of a single-bubble SL pulse from the wavelength of the emitted light suggests that bremsstrahlung may make a

substantial contribution to the total emission. Single-bubble SL results from quasi-adiabatic compression of the cavitation bubble and correlates with one of the versions of the thermal theory of cavitation (light emission of a black body, thermal bremsstrahlung, and emission caused by focusing of shock waves inside the bubble).

Alternative theories of single-bubble SL are now incompatible. The mechanisms of some effects occurring in single-bubble systems are yet to be clarified. Understanding these mechanisms will give a clearer insight into the nature of cavitation and may be helpful in developing a single-bubble acoustic chamber where thermonuclear reactions may be brought about.

The author is thankful to V L Ginzburg for his interest in this work and discussion of it, and to A G Molchanov and I M Margulis for many useful discussions.

The work is supported by a Copernicus grant (contract ERB IC 15-CT98-0808).

References

1. Frenzel H, Schultes H *Z. Phys. Chem.* **27** 421 (1934)
2. Walton A J, Reynolds G T *Adv. Phys.* **33** 595 (1984)
3. Zhuravlev A I, Akopyan V B *Ul'trazvukovoe Svechenie* (Ultrasound Luminescence) (Moscow: Nauka, 1977)
4. Margulis M A *Zvukokhimicheskie Reaktsii i Sonolyuminestsentsiya* (Sound-Induced Chemical Reactions and Sonoluminescence) (Moscow: Khimiya, 1986)
5. Mason T J, Lorimer J Ph *Sonochemistry: Theory, Application and Uses of Ultrasound in Chemistry* (London: Ellis Harwood, 1988)
6. Suslick K S (Ed.) *Ultrasound: Its Chemical, Physical, and Biological Effects* (New York: VCH, 1988)
7. Young F R *Cavitation* (New York: McGraw-Hill, 1989)
8. Margulis M A, in *Advances in Sonochemistry* (Ed. T J Mason) Vol. 1 (London: JAI Press, 1990) p. 39
9. Margulis M A *Sonochemistry and Cavitation* (London: Gordon & Breach, 1995)
10. Crum L A *Phys. Today* **47** (9) 22 (1994)
11. Barber B P et al. *Phys. Rep.* **281** 65 (1997)
12. Greenland P T *Contemp. Phys.* **40** 11 (1999)
13. Gaitan D F, Crum C C, Churh C C, Roy R A *J. Acoust. Soc. Am.* **91** 3166 (1992)
14. Harvey E N *J. Am. Chem. Soc.* **61** 2392 (1939)
15. Golubnichiĭ P I, Goncharov V D, Protopopov Kh V *Akust. Zh.* **15** 534 (1969)
16. Golubnichiĭ P I, Goncharov V D, Protopopov Kh V *Akust. Zh.* **16** 142, 338 (1970)
17. Margulis M A, Grundel' L M *Dokl. Akad. Nauk SSSR* **269** 405 (1983)
18. Kuttruff H *Acustica* **12** 230 (1962)
19. Margulis M A, Grundel' L M, Eskin G I, Shvetsov P N *Dokl. Akad. Nauk SSSR* **295** 1170 (1987)
20. Young R F *J. Acoust. Soc. Am.* **60** 100 (1976)
21. El'piner I E *Ul'trazvuk. Fiziko-khimicheskoe i Biologicheskoe Primenenie* (Ultrasound. Physico-Chemical and Biological Applications) (Moscow: Fizmatgiz, 1963) [Translated into English: Ultrasound: Physical, Chemical, and Biological Effects (New York: Consultants Bureau, 1964)]
22. Crum C C, Reynolds G T *J. Acoust. Soc. Am.* **78** 137 (1985)
23. Barber B P, Putterman S J *Nature* (London) **352** 318 (1991)
24. Flynn H G, in *Physical Acoustics. Principles and Methods* (Ed. W P Mason) Vol. 1, Pt. B *Methods and Devices* (New York: Academic Press, 1964) [Translated into Russian (Moscow: Mir, 1967) p. 7]
25. Smorodov E A, Kurochkin A K, Valitov R B, Margulis M A *Zh. Fiz. Khim.* **60** 893 (1986)
26. Didenko Yu T, Pugach S P, Gordeĭchuk T V *Opt. Spektr.* **80** 913 (1996) [*Opt. Spectrosc.* **80** 821 (1996)]
27. Margulis M A, in *3rd Meeting of the European Society of Sonochemistry, Portugal* (1993) p. 12
28. Taylor K J, Jarman P D *Aust. J. Phys.* **29** 319 (1970)
29. Flint E B, Suslick K S *J. Am. Chem. Soc.* **111** 6987 (1989)
30. Suslick K S, Flint E B *Nature* (London) **330** 554 (1987)
31. Smorodov E A, Kurochkin A K, Valitov R B, Margulis M A *Zh. Fiz. Khim.* **60** 648 (1986)
32. Margulis M A, Grundel' L M *Dokl. Akad. Nauk SSSR* **269** 405 (1983)
33. Peterson F B, Anderson T P *Phys. Fluids* **10** 4 (1967)
34. Demin S A, Verbanov V I, Margulis M A *Zh. Fiz. Khim.* **64** 3357 (1990)
35. Marinesco N, Trillat J *C. R. Acad. Sci.* **196** 858 (1933)
36. Gunther P, Heim E, Borgstedt H *Z. Elektrochem.* **61** 43 (1959)
37. Srinivasan D, Holroyd L V *J. Appl. Phys.* **32** 446 (1961)
38. Didenko Yu T, Pugach S P, Gordeĭchuk T V *Opt. Spektr.* **80** 913 (1996) [*Opt. Spectrosc.* **80** 821 (1996)]
39. Didenko Yu T et al. *Ultrasonics* **32** 71 (1994)
40. Taylor K J, Jarman P D *J. Am. Chem. Soc.* **93** 257 (1971)
41. Sehgal C, Sutherland R G, Verral R E *J. Phys. Chem.* **84** 529 (1980)
42. Sehgal C, Sutherland R G, Verral R E *J. Phys. Chem.* **84** 388 (1980)
43. Sehgal C, Sutherland R G, Verral R E *J. Phys. Chem.* **84** 396 (1980)
44. Sehgal C, Steer R P, Sutherland R G, Verral R E *J. Phys. Chem.* **81** 2618 (1977)
45. Kuhns D V, Brodsky A M, Burges L W *Phys. Rev. E* **57** 1702 (1998)
46. Breene R G J *Rev. Mod. Phys.* **29** 94 (1957)
47. Landau L D, Lifshitz E M *Elektrodinamika Sploshnykh Sred* (Electrodynamics of Continuous Media) (Moscow: Fizmatgiz, 1957) [Translated into English (Oxford: Pergamon Press, 1960)]
48. Margulis M A, Dmitrieva A F *Zh. Fiz. Khim.* **56** 875 (1982)
49. Matula T J, Roy R A *Ultrasonics Sonochemistry* **4** 61 (1997)
50. Crum C C, in *Ultrasonics World Congress 1995* Vol. 1 (Berlin, 1995) p. 63
51. Lepoint T et al. *J. Acoust. Soc. Am.* **101** 2012 (1997)
52. Flint E B, Suslick K S *J. Am. Chem. Soc.* **111** 6987 (1989)
53. Lambrecht A, Jackel M-T, Reynaud S *Phys. Rev. Lett.* **78** 2267 (1997)
54. Hiller R, Putterman S J, Weninger K R *Phys. Rev. Lett.* **80** 1990 (1998)
55. Noltingk B E, Neppiras E A *Proc. Phys. Soc.* **63B** 674 (1950)
56. Griffing V, Sette D *Phys. Rev.* **57** 234 (1952)
57. Jarman P D *J. Acoust. Soc. Am.* **32** 1459 (1960)
58. Ebeling K J *Proc. Soc. Photo-Optic Instrum. Eng.* **136** 348 (1977)
59. Lauterborn W, Ohl C-D *Ultrasonics Sonochemistry* **4** 65 (1997)
60. Rayleigh Lord *Phil. Mag.* **34** 94 (1917)
61. Plesset M S, Chapman B B *J. Fluid Mech.* **47** 283 (1971)
62. Akulichev V A, in *Moshchnye Ul'trazvukovye Polya* (High-Power Ultrasound Fields) (Ed. L D Rozenberg) (Moscow: Nauka, 1968) p. 129 [Translated into English: *High-Intensity Ultrasonic Fields* (New York: Plenum Press, 1971)]
63. Margulis M A, Maksimenko N A *Dokl. Akad. Nauk SSSR* **319** 656 (1991)
64. Cole R H *Underwater Explosions* (Princeton: Van Nostrand, 1948) [Translated into Russian (Moscow: IL, 1950)]
65. Keller J B, Miksis M *J. Acoust. Soc. Am.* **68** 628 (1980)
66. Prosperetti A, Lezzi A *J. Fluid Mech.* **168** 457 (1986)
67. Prosperetti A, Crum L A, Commander K W *J. Acoust. Soc. Am.* **83** 502 (1988)
68. *Proc. 1st Int. Conf. on Cavitation and Inhomogeneities* in *Underwater Acoustics* held on July 9–11, 1979 in Cöttingen, FRG (Ed. W Lauterborn) (Springer Series in Electrophysics 4) (Berlin: Springer-Verlag, 1980)
69. Grivnin Yu F, Zubrilov S P, Larin V A *Zh. Fiz. Khim.* **54** 56 (1980)
70. Prosperetti A, Seminara G *Phys. Fluids* **21** 1465 (1978)
71. Margulis M A, Dmitrieva A F *Zh. Fiz. Khim.* **71** 1149 (1997)
72. Lofstedt R, Barber B P, Putterman S J *Phys. Fluids A* **5** 2911 (1993)
73. Sehgal C M, Verral R E *Ultrasonics* **20** 37 (1982)
74. Margulis M A *Zh. Fiz. Khim.* **59** 1497 (1985)
75. Zarembo L K, in *Moshchnye Ul'trazvukovye Polya* (High-Power Ultrasound Fields) (Ed. L D Rozenberg) (Moscow: Nauka, 1968) p. 87 [Translated into English: *High-Intensity Ultrasonic Fields* (New York: Plenum Press, 1971)]
76. Margulis M A, Zubrilov S P *Zh. Fiz. Khim.* **58** 483 (1984)
77. Margulis M A, Grundel' L M *Zh. Fiz. Khim.* **56** 1941 (1982)
78. Hoyt J W, Taylor J J *J. Fluids Eng.* **103** 14 (1981)
79. Shalnev K K, Shalobasov I A, Kozirev C P, Haldeev E V *Proc. 5th Congr. Fluid Machinery* **2** 1021 (Budapest, 1975)

80. Margulis M A, in *Advances in Sonochemistry* Vol. 1 (Ed. T J Mason) (London: JAI Press, 1990) p. 39
81. Margulis M A *Zh. Fiz. Khim.* **71** 1885 (1997)
82. Turkovskaya N V, in *Proc. All-Union Symp. Acoustical Cavitation and Problems of Intensification of Technological Processes, Odessa, 1989* (Odessa, SI-17, 1989) p. 23
83. Margulis M A, Margulis I M *Zh. Fiz. Khim.* **71** 1890 (1997)
84. Bortnik I M, Vereshchagin I P, Vershinin Yu N *Electrofizicheskie Osnovy Tekhniki Vysokikh Napryazheniĭ* (Electrophysical Foundations of High-Voltage Techniques) (Moscow: Energoatomizdat, 1993)
85. Margulis M A, Margulis I M *Zh. Fiz. Khim.* **72** 556 (1998)
86. Stratton J A *Electromagnetic Theory* (New York: McGraw-Hill, 1941) [Translated into Russian (Moscow: Gostekhizdat, 1948)]
87. Margulis M A, Grundel' L M *Zh. Fiz. Khim.* **55** 687 (1981)
88. Golubnichiĭ P I, Goncharov V D, Protopopov Kh V *Akust. Zh.* **15** 534 (1969)
89. Hiller R, Putterman S J, Barber B P *Phys. Rev. Lett.* **69** 1182 (1992)
90. Weninger K R et al. *J. Phys. Chem.* **99** 1495 (1995)
91. Gordeychuk T V, Didenko Yu T, Suslick K S, in *Proc. 6th Meeting of European Society of Sonochemistry* (Rostock, 1998) p. 60
92. Ciuti P, Dezhkunov N V, Francescutto A, Iernetti G, in *Proc. ASME Fluids Eng. Division Summer Meeting, June 22–26* (1997)
93. Lohse D et al. *Phys. Rev. Lett.* **78** 1359 (1997)
94. Zel'dovich Ya B, Raĭzer Yu P *Fizika Udarnykh Voln i Vysokotemperaturnykh Gidrodinamicheskikh Yavleniĭ* (Physics of Shock Waves and High-Temperature Hydrodynamic Phenomena) (Moscow: Fizmatgiz, 1965) [Translated into English (New York: Academic Press, 1966–1967)]
95. Margulis M A, in *Ultrasonics World Congress 1995* Vol. 2 (Berlin, 1995) p. 639
96. Margulis M A *Akust. Zh.* **22** 261 (1976)
97. Rozenberg L D, Sirotyuk M G *Akust. Zh.* **5** 206 (1959)
98. Rozenberg L D, Sirotyuk M G *Akust. Zh.* **9** 61 (1963)
99. Margulis M A, Margulis I M, in *Proc. 15th Int. Symposium on Nonlinear Acoustics, Cöttingen, September 1999* (Göttingen, 1999)
100. Margulis M A, RF Patent No. 2096934 (1995)
101. Young J B, Schmidel T, Woowon Kang *Phys. Rev. Lett.* **77** 4816 (1996)
102. Margulis M A, Grundel' L M *Zh. Fiz. Khim.* **56** 2987 (1982)
103. Golubnichiĭ P I, Goncharov V D, Protopopov Kh V *Khim. Vys. Energ.* **3** 515 (1969)
104. Bronshteĭn R M, Paukov Yu N, Bologa M K *Izv. Akad. Nauk Mold. SSR. Ser. Tekh.* (1) 47 (1973)
105. Gimenez C, Goby F, in *Proc. 1st Int. Conf. on Cavitation and Inhomogeneities* in *Underwater Acoustics* held on July 9–11, 1979 in Cöttingen, FRG (Ed. W Lauterborn) (Springer Series in Electrophysics 4) (Berlin : Springer-Verlag, 1980) p. 101
106. Saksena T K, Nyborg W L *J. Chem. Phys.* **53** 1722 (1970)
107. Kolbanovskiĭ Yu A *Impul'snoe Szhatie Gazov v Khimii i Tekhnologii* (Pulse Compression of Gases in Chemistry and Technology) (Moscow: Nauka, 1982)
108. Margulis M A, Gavrilov V A *Zh. Fiz. Khim.* **65** 588 (1991)
109. Margulis M A, Dmitrieva A F *Zh. Fiz. Khim.* **66** 1409 (1992)
110. Henglein A, in *Advances in Sonochemistry* (Ed. T J Mason) Vol. 3 (London: JAI Press, 1993) p. 17
111. Margulis M A *Zh. Fiz. Khim.* **52** 605 (1978)
112. Smorodov E A, Kurochkin A K, Valitov R B, Margulis M A *Zh. Fiz. Khim.* **60** 1234 (1986)
113. Schwinger J *Proc. Natl. Acad. Sci. USA* **89** 4091 (1992)
114. Eberlein C *Phys. Rev. Lett.* **76** 3842 (1996)
115. Eberlein C *Phys. Rev. A* **53** 2772 (1996)
116. Unnikrishnan C S, Mukhopadhyay S *Phys. Rev. Lett.* **77** 4690 (1996)
117. Garcia N, Levanyuk A P *Phys. Rev. Lett.* **78** 2268 (1997)
118. Esquivel-Sirvent R, Jauregui R, Villareal C *Phys. Rev. A* **56** 2463 (1997)
119. Mohanty P, Khare S V *Phys. Rev. Lett.* **80** 189 (1998)
120. Frommhold L, Atchley A A *Phys. Rev. Lett.* **73** 2883 (1994)
121. Prosperetti A *J. Acoust. Soc. Am.* **101** 2003 (1997)
122. Lepoint T, Mullie F *Ultrasonics Sonochemistry* **1** 13 (1994)
123. Margulis M A *Akust. Zh.* **15** 153 (1969)
124. Wu C C, Roberts P H *Phys. Rev. Lett.* **70** 3424 (1993)
125. Gompf B, Gunte R, Nick G, Pecha R, Eisenmenger W *Phys. Rev. Lett.* **79** 1405 (1997)
126. Margulis M A *Ultrasonics* **25** 157 (1985)
127. Moss W C, Clarke D B, White J W, Young P A *Phys. Fluids A* **6** 2979 (1994)
128. Lee Y P, Kahng S W, Jeon J S, Kwak H-Y *J. Phys. Soc. Jpn.* **66** 2537 (1997)
129. Golubnichiĭ P I, Goncharov V D, Protopopov Kh V *Akust. Zh.* **16** 338 (1970)
130. Levshin V N, Rzhevkin S N *Dokl. Akad. Nauk SSSR* **16** 407 (1937)
131. Frenkel' Ya I *Zh. Fiz. Khim.* **14** 305 (1940)
132. Margulis M A *Zh. Fiz. Khim.* **55** 154 (1981)
133. Degrois M, Baldo P *Ultrasonics* **12** 25 (1974)
134. Hiller R, Weninger K, Putterman S J, Barber B P *Science* **266** 248 (1994)
135. Chou T, Blackman E G *Phys. Rev. Lett.* **76** 1549 (1996)
136. Vincenti M G, Kruger H *Introduction to Physical Gas Dynamics* (New York: Krieger Publ., 1965)
137. Delgadino G A, Bonetto F J *Phys. Rev. E* **56** R6248 (1997)
138. Hickling R, Plesset M S *Phys. Fluids* **7** 7 (1964)
139. Glasstone S, Lovberg R H *Controlled Thermonuclear Reactions* (New York: Van Nostrand, 1960)
140. Margulis M A *Zh. Fiz. Khim.* **50** 1 (1976)
141. Plesset M S, Zwick S A *J. Appl. Phys.* **25** 493 (1954)
142. Margulis I M, Margulis M A *Zh. Fiz. Khim.* **74** (2000) (in press)
143. Moran M J et al. *Nucl. Instrum. Methods Phys. Res., Sect. B* **96** 651 (1995)
144. Lohse D et al. *Phys. Rev. Lett.* **78** 1359 (1997)
145. Margulis I M, Margulis M A *Zh. Fiz. Khim.* **74** 561 (2000)
146. Brueckner K A, Jorna S *Laser Driven Fusion* (Michigan: Ann Arbor, 1973) [Translated into Russian (Moscow: Atomizdat, 1977)]
147. Margulis M A, Dmitrieva A F *Zh. Fiz. Khim.* **56** 875 (1982)
148. Jarman P D *J. Acoust. Soc. Am.* **32** 1459 (1960)
149. Hickling R, Plesset M S *Phys. Fluids* **7** 1 (1964)
150. Flint E B, Suslick K S *Science* **253** 1397 (1991)
151. Yasui K *Phys. Rev. E* **56** 6750 (1997)
152. Guth M *Acustica* **5** 526 (1956)
153. Margulis M A, Margulis I M *Ultrasonics Sonochemistry* **6** 15 (1999)
154. Kwak H-Y, Na J H *J. Phys. Soc. Jpn.* **66** 3074 (1997)
155. Weninger K R et al. *Phys. Rev. E* **56** 6745 (1997)
156. Taylor K J, Jarman P D *J. Am. Chem. Soc.* **93** 257 (1971)
157. Arakeri V H *Prama J. Phys.* **40** L145 (1993)
158. Tsiklauri D *Phys. Rev. E* **56** R6245 (1997)
159. Grivnin Yu A, Zubrilov S P, Larin V A *Zh. Fiz. Khim.* **54** 56 (1980)
160. Barber B P, Putterman S J *Phys. Rev. Lett.* **69** 3839 (1992)
161. Barber B P et al. *J. Acoust. Soc. Am.* **91** 3061 (1992)
162. Gompf B, Eisenmenger W *Phys. Rev. B* **54** (3) 231 (1998)
163. Putterman S J *Phys. World* (May) 38 (1998)
164. Margulis M A *Ultrasonics* **23** 157 (1985)
165. Vogan P W, Leeman S *Acustica* **59** 1722 (1970)
166. Yuan L, Cheng H Y, Chu M-C, Leung P T *Phys. Rev. E* **57** 4265 (1998)
167. Moss W C et al. *Phys. Rev. E* **59** 2986 (1999)
168. Plesset M S *Bubble Dynamics. Cavitation in Real Fluids* (New York: 1965)
169. Raĭzer Yu P *Fizika Gazovogo Razryada* (Gas Discharge Physics) (Moscow: Nauka, 1987) [Translated into English (Berlin: Springer-Verlag, 1991)]
170. Giri A, Arakeri V H *Phys. Rev. E* **58** R2713 (1998)
171. Cheng H Y, Chu M-C, Leung P T, Yuan L *Phys. Rev. E* **58** R2705 (1998)
172. Hingelfeldt S, Grossman S, Lohse D *Nature* (London) **398** 402 (1999)
173. Gavrilov L R, in *Fizicheskie Osnovy Ul'trazvukovoĭ Tekhnologii* (Physical Principles of Ultrasonic Technology) (Ed. L D Rozenberg) (Moscow: Nauka, 1970) p. 393 [Translated into English (New York: Plenum Press, 1973)]
174. Guderley G *Luftfahrtforschung* **19** 302 (1942)
175. Tsiklauri D *Phys. Rev. E* **56** 6245 (1997)
176. Smorodov E A, Kurochkin A K, Valitov R B, Margulis M A *Zh. Fiz. Khim.* **60** 648 (1986)
177. Suslick K S, in *Proc. Intern. Symposium on Nonlinear Acoustics, Göttingen, September 1–4, 1999*

178. Johnson M L, Nicol M, Holmes N C, in *Shock Waves in Condensed Matter* (Ed. Y M Gupta) (New York: Plenum Press, 1986) p. 201
179. Plesset M S *Bubble Dynamics. Cavitation in Real Fluids* (New York: 1965)
180. Yasui K *Phys. Rev. E* **60** 1754 (1999)
181. Yasui K *Phys. Rev. E* **60** 1759 (1999)
182. Sochard S, Wilhelm A-M, Delmas H *Ultrasonics Sonochemistry* **4** 77 (1997)
183. Matula T J et al. *Phys. Rev. Lett.* **75** 2602 (1995)
184. Akulichev V A *Kavitatsiya v Kriogennykh i Kipyashchikh Zhidkostyakh* (Cavitation in Cryogenic and Boiling Fluids) (Moscow: Nauka, 1978) p. 216